# THE INFLUENCE OF COMPETITION BETWEEN SELENATE AND METASILICATE IONS ON THEIR MIGRATION BEHAVIOR IN BENTONITE

NERA research group, Reactor Institute Delft, TU Delft

BSc Thesis Philippe Carter

## ABSTRACT

In this thesis we focused on the competition between selenium oxyanions and metasilicate on their migration behavior in the context of deep geological storage of high-level nuclear waste. Se is considered as highly mobile and silicates can be abundantly present as the results of corrosion of concrete engineered structures. With the intention of performing the migration experiments within a reasonable time scale an electromigration technique was applied.

**The influence of competition between selenium and metasilicate ions on their migration behavior in bentonite.**

Philippe Carter
4167449

**Bachelor thesis performed at:**

Section for Nuclear Energy & Radiation Applications
Reactor Institute Delft
Technical University Delft

**Under supervission of:**

Prof. Dr. J. Kloosterman
Dr. Denis Bykov

June 12th 2015

## LIST OF SYMBOLS

Superscript "a," for apparent, found throughout this thesis, means: as observed in porous medium, taking tortuosity and retardation into account.

| Symbol | Term | Unit | Value |
|---|---|---|---|
| $\alpha$ | Longitudinal dispersion | [m] | |
| D | Dispersion coefficient | [$m^2/s$] | |
| $D_m$ | Molecular diffusion coefficient | [$m^2/s$] | |
| *e* | Charge of an electron | [C] | $1{,}6*10^{-19}$ |
| E | Electrical field | [V/m] | |
| $E_h$ | Reduction potential | [V] | |
| $K_b$ | Boltzmann constant | [J/K] | $1{,}3806488*10^{-23}$ |
| $\mu$ | Viscosity | [$Ns/m^2$] | |
| $\mu_e$ | Ionic mobility | [$m^2/sV$] | |
| $Q_0$ | Initial concentration of activity | [Bq] | |
| r | Radius of a particle | [m] | |
| R | Retardation factor | [-] | |
| $R_d$ | Sorption distribution ratio | [L/kg] | |
| S | Surface area of clay sample | [$m^2$] | |
| $\tau$ | Tortuosity | [-] | >1 |
| t | Experimental time | [t] | |
| T | Temperature | K | |
| $\nu$ | Velocity | [m/s] | |
| $V_c$ | Convection velocity | [m/s] | |
| $\nu_{em}$ | Electromigration velocity | [m/s] | |
| $\nu_{eo}$ | Electroosmosis velocity | [m/s] | |
| *x* | Distance of actual diffusion path | [m] | |
| *z* | Distance of experimental end-to-end diffusion path | [m] | |
| Z | Valance of particle | [-] | Integer number |

## TABLE OF CONTENTS

# 1. INTRODUCTION

## 1.1. Overview of deep geological nuclear waste disposal

The only way that radioactive waste becomes fully unharmful is through decay, which in the case of long-living high-level nuclear waste (HLW) can take hundreds of thousands of years. Therefore it is necessary that HLW is isolated from the biosphere long enough for the radiotoxic elements to fully decay before having traveled enough distance to enter the biosphere. Underground storage is a proposed method of reducing health risks that high-level radioactive waste poses on society. The current management strategy for HLW for many countries, including the Netherlands, is temporary storage in aboveground facilities for about a hundred years [3]. Deep geological disposal in clay formations is one of the proposed methods of final storage that has been investigated since 1976.

In order to meet the objective of sufficient long-term subsurface isolation, a system of five complementary barriers (figure 1) has been designed which attempts to prevent underground waters, that could potentially have dissolved radionuclides, from carrying activity to the surface. The near field barriers, such as vitrified glass, a carbon steel overpack and cementitious backfill, are considered engineered barriers. The main goal of the engineered barriers is to prevent ground waters from reaching the radionuclides. The far field, natural

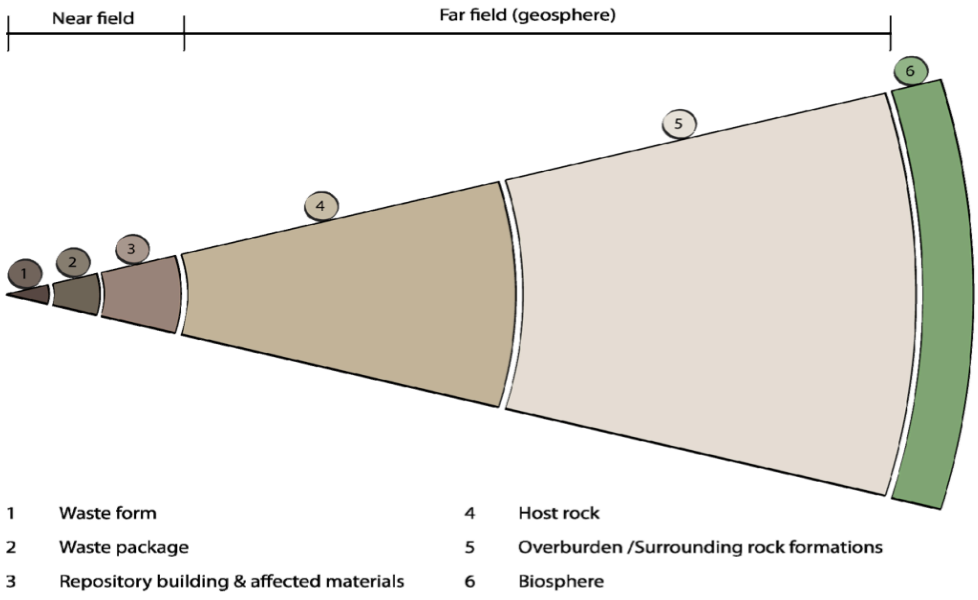


Figure 1: Schematic overview of five-layer barrier system for deep geological storage [1].

barriers consist of a host rock, such as clayey materials, and other rock formations.

Over time it is possible that the encapsulation of HLW partly fails due to mechanical disturbances, corrosion or other factors of nature. Radionuclides then have the opportunity to diffuse out of their canister. A backfill material is applied around the container to protect it from groundwater reaching the waste. The backfill also provides a moderately reducing environment to minimize container corrosion and also initially absorb the radionuclides if they manage to escape their canister [4].

## 1.2. Bentonite as a backfill material

Bentonite, a clay that consists mostly of montmorillonite [5], is considered to be a good candidate to serve as a backfill material because it (1) provides a low-permeable medium that limits radionuclide diffusion, (2) provides sorption capacity for radionuclides, (3) has an alkine pH between 8.5 and 9.0, which increases the adsorption capacity of the clay [6-8] and minimizes container corrosion [4] and (4) possesses a high plasticity. The clay has been intensively studied in the past as a backfill material around nuclear waste containers [4, 6, 9]. Bentonite deposits in Wyoming, USA make up 70% of the worlds supply and have a favorable sodium content for application in a nuclear waste repository. It contains 65-75% sodium rich phyllosilicate montmorillonite, 10-14% quartz, 5-9% feldspars, 3-5% carbonates and chlorite and 1-3% heavy metals [10]. Wyoming bentonite was used in this study.

### 1.2.1. Structure of bentonite

To understand the transport and sorption mechanisms in this specific type of clay, we have to look at the chemical structure of bentonite. Clay particles are made out of combinations of sheets of silica tetrahedrons and sheets of aluminum or magnesium

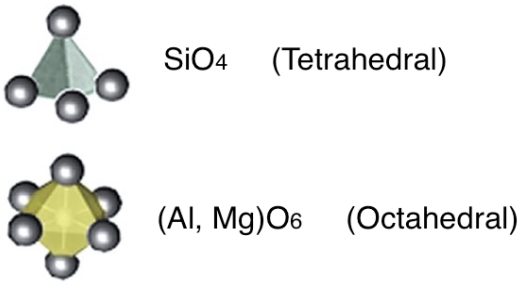


**Figure 2: Schematic view of polyhedral clay particles.**

octahedrons. These sheets are considered to be the building blocks of all clay minerals. Single polyhedras are shown in figure 2.

Four main clay mineral groups are identified by various stacking arrangements of these tetrahedron and octahedron sheets. A schematic overview is shown in figure 3 [7].

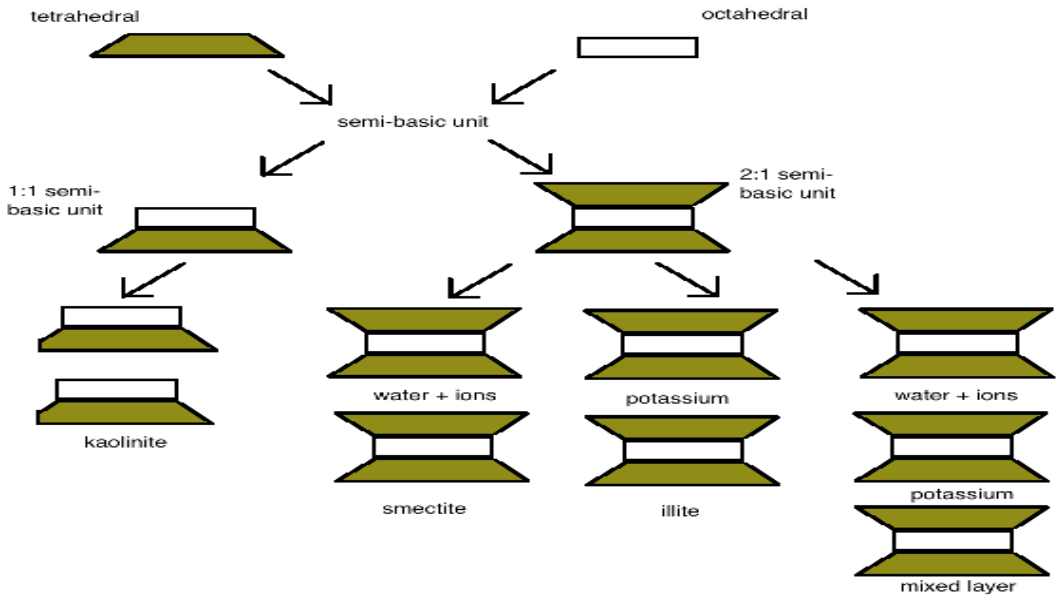


**Figure 3: Structural classification of clay minerals.**

Montmorillonite, the main component of bentonite, is a smectite mineral, giving it the so-called 2:1 TOT structure (tetrahedral - octahedral - tetrahedral) with aqueous interlayers. $Na^{+}$ and $Ca^{2+}$ ions that populate these interlayers can easily be hydrated giving bentonite its ability to swell. Figure 4 gives a clear picture of the two TOT layers with an interlayer in the middle.

A set of silicate layers and interlayers form a clay particle. These particles are irregularly shaped and cannot be neatly arranged. Due to the irregularity of the particles, pores are created within its macrostructure, which can contain water channels that support the transport of ions.

As seen in figure 4, the oxygen atoms from both tetrahedrons and octahedrons create an oxygen skeleton that holds the particles in place. The abundance of two oxygen atoms of every octahedron (red dots in figure 4) is the partial cause of the negative charge of the mineral sheets.

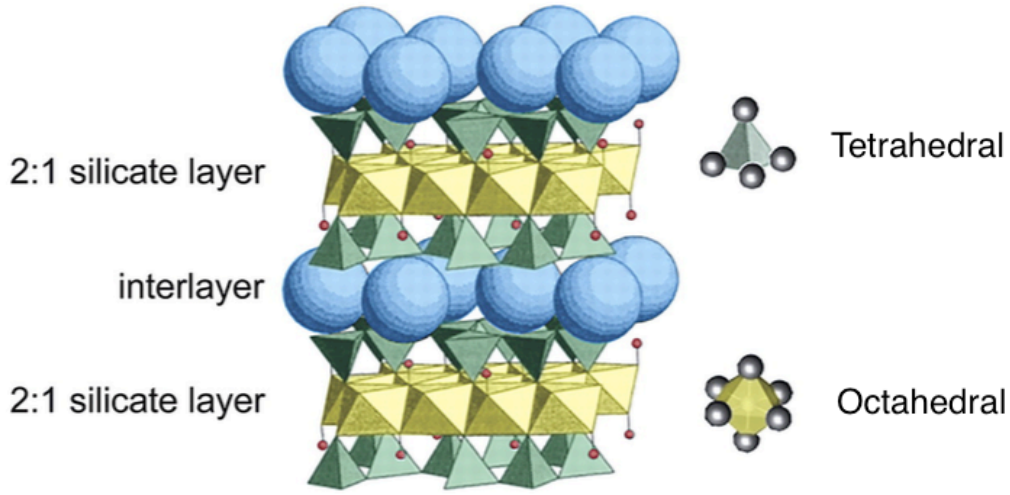


**Figure 4: Schematic representation of a two-layer type clay. The green pyramids represent the silica tetrahedrons. The yellow double pyramids represent the Al, Mg or Fe octahedrons. Red dots represent free oxygen atoms. The blue interlayers consist of water molecules and interlayer cations, e.g. $Na^{+}$ and $Ca^{2+}$.**

Isomorphous substitution, the ability of a crystal lattice to hold cations of suitable size other than normally found in the lattice, is the second reason why clay minerals are negatively charged. The Si atoms in the silicate layers can be exchanged by Al or any other atom with a lower valency (e.g. Mg). This exchange creates an excess negative charge in the clay structure.

As mentioned before, the interlayers in bentonite consist of water molecules. These molecules are attracted to the negative charge of the silicate layers and are able to form hydrogen bonds with the free oxygen atom. The thickness of the aqueous interlayer is influenced by two factors: (1) the concentration of cations in the solution and (2) the clay surface itself. Cations that are in contact with water become hydrated and cations that are in close proximity of the surface can use water for their hydration shell. This shell can be several water molecules thick, depending on the charge of the cation.

When water approaches the clay surface, its properties change. The closer water molecules are to the surface, the denser the solution. This creates a higher viscosity near the clay surface. The first water layer may be 100 times more viscose than free water. In addition, water that is absorbed by the clay surface

loses a degree of freedom. They can move freely in the direction parallel to the surface, but not perpendicular to or away from the surface [11, 12].

### 1.2.2. Transport of ions through bentonite

If interlayers become too thick, ions that are solved in the aqueous interlayers are able to use groundwater flow to migrate through the clay pores. This is an undesirable event in the case of radionuclide containment. Bentonite, however, has been proven to be a suitable clay formation and it can therefore be assumed that the transport of ions is controlled by diffusion and not by convection. The molecular diffusion coefficient, $D_m$ [$m^2/s$], is the most important parameter determining the diffusion behavior of an ion. It states the velocity at which a nuclide travels through clay and it is dependent on the sorption properties of that clay (see section 1.3.).

Ion mobility in natural deep groundwater/host rock formations is subjected to a set of opposing chemical mobilizing and immobilizing reactions (figure 5). The net effect will eventually determine the mobility of each ion in clayey soils.

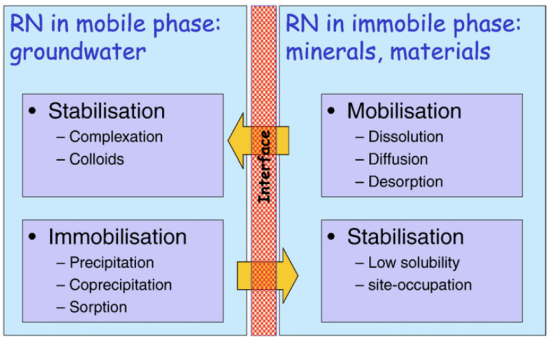


**Figure 5: Schematic view of mobilising and immobilising reactions governing radionulcie mobility in natural environments [2].**

An important characteristic of a mobile radionuclide is its very low $R_d$ value. The $R_d$ value ($R_d$={RN}/[RN]) is a distribution ratio for the concentration of radionuclide RN, were {} indicates concentration on the solid and [] indicates concentration in solution (in mol/L). Safety experts often assume zero retention for a radionuclide that is considered very mobile. This assumption is not entirely correct. A slight difference in a low $R_d$ value can still have a significant effect over a long distance of some tens to hundreds of meters. In clay rock for example, an $R_d$ value of only 0.1 L/kg will increase the break through time of anions with a diffusion coefficient of $5*10^{-12}$ $m^2/s$ over a distance of 50m with 560000 years [2].

## 1.3. Sorption processes in bentonite

Literature data state that the sorption capabilities of clays mainly result from the negative charge of the clay surface. The charge gives clay minerals the capability to adsorb positively charged ions. The high surface area and high porosity of clays also contribute to the good sorption properties of clay. Montmorrillonites, like bentonite, have the largest surface area and a high cation exchange capacity (see section 1.3.1.) among clays and are therefore considered to be good sorbers [13].

### 1.3.1. Cation exchange capacity

The cation exchange capacity (CEC) of a clay mineral is defined by "the amount of exchangeable cations per dry weight that a clay mineral is capable of holding and that are available for exchange". This quantity of exchangeable cations is expressed in milliequivalents per 100 gram. Isomorphous substitution (see section 1.2.1.) is one of the factors contributing to the CEC. The excess charge resulting from isomorphous substitution attracts cations onto the clay surface. A high pH also contributes to a higher CEC. Increasing pH can ionize the edges of the silicate sheets. These negative charges also have to be compensated by cations from the interlayer [14].

### 1.3.2. Diffuse double layer

In aqueous medium, the negative charge of clay minerals (explained in section 1.2.1.) induces a diffuse double layer (figure 6a). To obtain electrical neutrality, the charge of the clay minerals is compensated by nearby cations. Accordingly, anions are repelled from the clay surface. The charged surface of the clay and the water layer right next to the clay surface with an excess of cations, creates the diffuse double layer. At a relatively large distance from the clay surface, the concentrations of cations and anions are in equilibrium [7].

In transport processes, compressed clay layers work as a semipermeable membrane. Tuwiner defined semipermeablity as "the ability to permit the transport of some components of a solution while others are excluded from transport [15]. Due to overlapping diffuse double layers in compressed clay (figure 6b), anions that attempt to migrate through the, otherwise in equilibrium,

part of the aqueous interlayer are repelled by the negative charge of the clay particles. To maintain electrical neutrality in the solution, cations will remain with their counter-ions and thus their movement through the clay will also be retained [16].

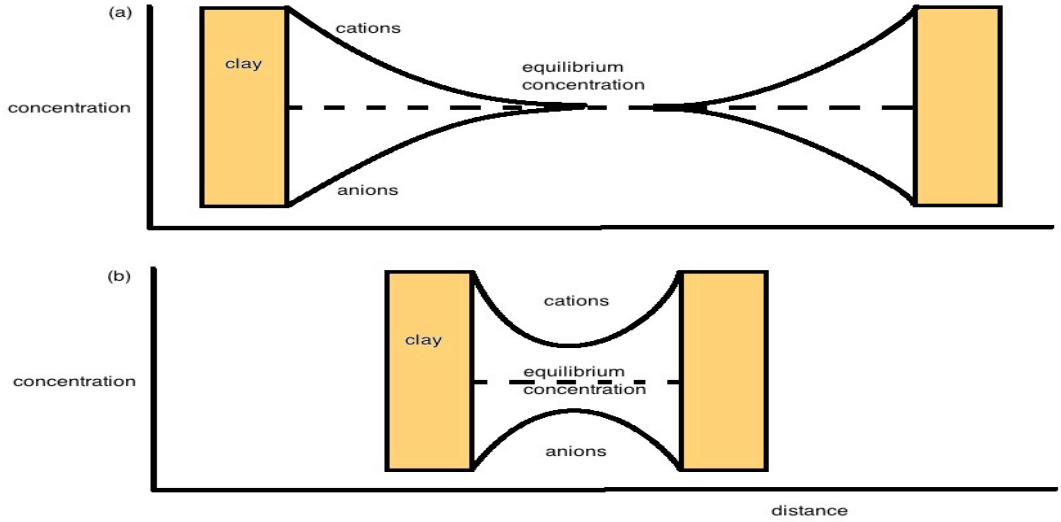


**Figure 6: Distribution of cations and anions in the near area of clay sheets. The dispersed situation is shown in (a) were the diffuse double layers of the clay particles don't overlap. Under an overburden pressure, shown in (b), the clay sheets are forced closer together which results in an overlap of their diffuse double layers [7].**

## 1.4. Deriving migration coefficients in the laboratory

Different techniques are used in laboratories for determining migration parameters of nuclides. Pure diffusion experiments are founded solely on the principle of a concentration gradient. Dispersion/advection experiments add a hydraulic pressure gradient to the set-up. This slightly decreases the experimental time. A third method is electromigration. Here a potential is applied over the sample attracting ions to either the anode or the cathode.

The key advantage of electromigration over the other techniques is its relatively very short experimental time. The disadvantage however is that only the apparent molecular diffusion coefficient can be derived experimentally. Pure diffusion and dispersion/advection experiments also allow the porosity and retardation factor to be determined. Because of the short experimental time and the low hydraulic conductivity of Bentonite, the experiments in this thesis were conducted with an electromigration set-up [17].

## 1.5. Selenium and cesium in the context of nuclear geological disposal

This section covers the research elements for this thesis. The first part will cover the relevance of the elements that have been researched; the second part focuses on the chemistry of both elements.

### 1.5.1. Potentially dangerous isotopes

When disposing nuclear waste in clayey materials it is anticipated that the man made barriers eventually wear and tear or lose their function due to an accident and that isotopes might be released into the host rock formation. In the case of failing encapsulation, most isotopes only migrate a few centimeters in the sediment before they decay. A few long-living radionuclides however, are mobile enough to potentially reach the biosphere and threaten society with long-term exposure. Marivoet and Weetjens stated that fission and activation products such as $^{129}I$, $^{79}Se$, $^{135}Cs$ or $^{126}Sn$ are of primary concern due to the fact that for these isotopes, other than for the actinides, migration times and distances can be large [2, 18]. This thesis will focus on two radionuclides of interest, namely $^{79}Se$ and $^{135}Cs$.

Marivoet and Weetjens have stated that "$^{79}Se$ is a main contributor to the total dose in the case of disposal of vitrified HLW" [18]. Although its fission yield of 0.04% is low, it can be found at noteworthy levels in spent nuclear fuel and in fuel reprocessing waste materials [19]. It is also potentially more dangerous than other isotopes due to the fact that selenium is an essential micronutrient for many organisms and is therefore likely to be absorbed into the food chain [20].

$^{137}Cs$ is one of the two medium-lived fission products, $^{135}Cs$ is a long-lived fission product. Therefore these two isotopes account for a large portion of the radioactivity in spent nuclear fuel. Moreover cesium is a well-researched element, which means that there is a wealth of information available for comparison. The isotope was only used to validate the experimental setup by comparing results to previously conducted research.

### 1.5.2. Chemistry of selenium

$^{79}$Se is a pure β$^-$-emitter that disintegrates directly to the ground state level of $^{79}$Br. Its half-life time has never been documented correctly and estimates reach from 65000 to 1.1 million years. Recent research has determined the half-life time of $^{79}$Se to be 377000 years [19] and 327000 years [21]. The geochemical behavior of selenium in clay is mostly controlled by abiotic chemical reactions. Microbial activity in the very compact deep-ground bentonite is expected to be close to zero and is therefore disregarded.

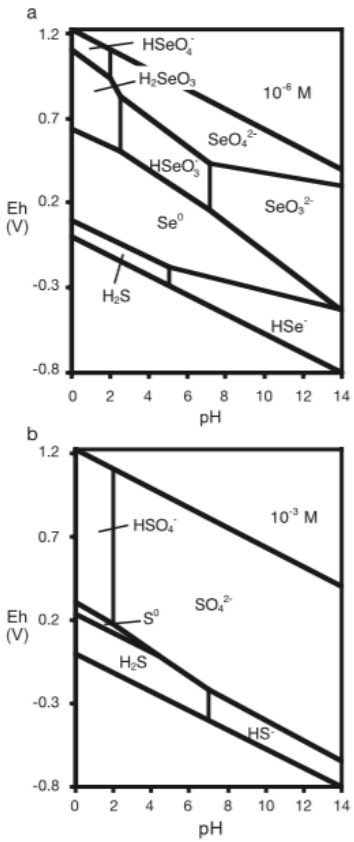


**Figure 7: Eh-pH graph of speciation of (a) selenium and (b) Sulfur.**

Selenium belongs to group 16 of the periotic table. The electron configuration of selenium is given by [Ar]3d$^{10}$4p$^4$4s$^2$. In the periodic table, it lies between sulfur and tellurium and resembles sulfur quite closely in its oxidation states, but is a little more complex than sulfur. Figures 7a and b, the Eh-pH diagrams of sulfer and selenium, show several similarities and differences. Selenium forms selenites, which are similar to sulfides. The most common oxidation forms of selenium are $Se^{2-}$, $Se_{(s)}$, $Se^{4+}$ and $Se^{6+}$. Figure 7a shows the oxidation states of selenium under different pH and Eh conditions. The tretra- and hexavalent states are usually bound to oxygen, creating selenite ($SeO_3^{2-}$) and selenate ($SeO_4^{2-}$). In acidic solutions $H^+$ may be bound to the anions. The redox potentials of selenium are reported below [22, 23]:

Acidic solutions:

$$H_2Se \xrightarrow{-0.40V} Se^0 \xrightarrow{+0.74V} SeO_3^{2-} \xrightarrow{+1.15V} SeO_4^{2-}$$

Alkine solutions:

$$Se^{2-} \xrightarrow{+0.92V} Se^o \xrightarrow{+0.366V} SeO_3^{2-} \xrightarrow{+0.05V} SeO_4^{2-}$$

Under slightly reducing conditions, Se(IV) is the main aqueous oxidation state. Under bentonite conditions however (pH 8 - 10, Eh around -300 mV), selenium is expected as the $HSe^-$ species. Nevertheless, the oxidation state at which it comes out of the nuclear waste is unknown and likely to hold selenite or selenate as well [2]. Especially selenate is known to have very poor retardation properties [24]. Diffusion experiments have shown that oxidation or reduction processes do not always comply with the expected pattern. Beauwens et al., for example, noticed that selenate ions were not reduced along their migration path in reducing Boom Clay, even though Se(IV) or Se(-II) were thermodynamically favored in those conditions [25].

Due to the slow oxidation/reduction properties of selenium, the (IV) and (VI) configuration of selenium are of particular interest. Selenate can be formed by strong oxidizing agents like hydrogen peroxide or by applying enough potential at the right pH in an oxygen rich environment [22, 25]. The reduction back to a lower oxidation state is a very slow process [2]. Reduction from (IV) to elemental selenium however is a simple and quick process using a reducing agent like thiourea ($CH_4N_2S$). The oxidizing and reducing reactions are shown below [22, 26]:

reduction:

$$SeO_3^{2-} + thiourea \longrightarrow Se^0$$

oxidation:

$$SeO_3^{2-} + H_2O_2 \longleftrightarrow SeO_4^{2-} + H_2O$$

$$NaSeO_3 + H_2O \xrightarrow{electricity} NaSeO_4 + H_2$$

Selenium oxyanions are known to form a mixture of inner- and outer-sphere complexes on ironhydroxides ($Fe(OH)_3$) and aluminumhydroxides ($Al(OH)_3$) rich surfaces [27]. The iron or aluminum atoms in the clay attract oxyanion-ligands. A

hydroxyl group of the metalhydroxide is replaced by selenite or selenate. The formation of inner-spheres is given by the reactions below:

$$SeO_3^{2-} + FeOH \rightarrow FeSeO_3^- + OH^-$$
$$HSeO_3^- + FeOH \rightarrow FeSeO_3^- + H_2O$$

An acidic environment facilitates the expulsion of the hydroxyl group, as the $OH^-$ is quickly protonated. The expulsion of neutral water is energetically favored. In bentonite however, conditions are alkaline and only allow for selenite to form complexes. This is believed to be one of the reasons for the low adsorption of selenate [27]. The formation of outer-sphere complexes, which are not covantly bond to iron or aluminum, but instead use hydrogen bonding, is possible for selenate. This form of retention, however, is very weak compared to inner-sphere complexes [28].

Oxyanions can form monodentate, mononuclear and bidentate bonded inner-sphere complexes (see figure 8).

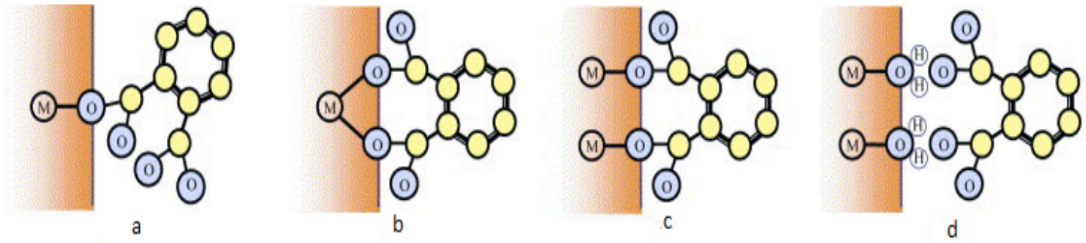


**Figure 8: Schematic overview of surface complex structures. (a) Monodentate inner-sphere complex. (b) Mononuclear inner-sphere complex. (c) Bidentate inner-sphere complex. (d) outer-sphere complex.**

### 1.5.3. Chemistry of cesium

$^{135}Cs$ and $^{137}Cs$ are both $\beta^-$-emitters. $^{135}Cs$ has a half-life time of 2300000 years and is considered long-lived, whereas $^{137}Cs$ has a half-life time of 30 years and is considered medium-lived.

Cesium is a soft alkali metal with a melting point of 28 °C. This makes it one of the five elemental metals that are liquid near room temperature. Cesium's redox chemistry is much simpler than selenium. Just like the other alkali metals,

cesium is very reactive and only has one oxidation state besides elemental cesium: +1 (see figure 9). The $Cs^+$ cation can bind to a diverse range of anions.

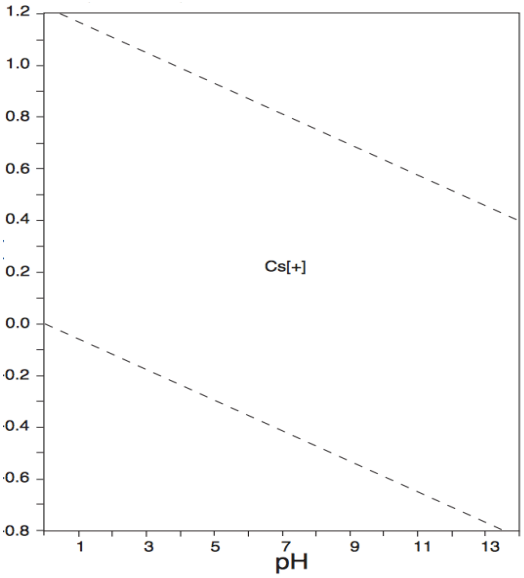

Figure 9: Eh-pH speciation of cesium.

Cation exchange (see section 1.3.1.) is the largest and most important contributing factor to the retardation of Cesium in bentonite. The negatively charged clay surface sorbs the positive cesium ions to compensate for the net negative charge of the clay particle.

## 1.6. Influence of competition

Over the past decades there has been a lot of research on the apparent mobility and the apparent molecular diffusion coefficient of long-lived radionuclides in clayey soils like boom clay and bentonite. This previous research has focused on the mobility of single elements through a medium. This thesis will concentrate more on the influence of competition between two elements or ionic species on their apparent mobility.

Certain elements or ionic species are thermodynamically favored to be absorbed by the clay surface. Different compounds that are retained by the same geochemical processes are likely to compete for sorption site in the clay. Similar cations, for example, may be competing over a limited amount of exchangeable cations as they are both retained predominantly by CEC. A second type of competition could arise between different oxidation states (e.g. Se(IV) and Se(VI)) of one element. A third contributor to this problem might be oxyanions of one element that compete with oxyanions of another element as they both form similar inner- and outer-sphere complexes.

### 1.6.1. Previous research

Electromigration experiments were conducted by Zappey at the Reactor Institute of TU Delft (RID) [29]. A discrepancy between the distribution profiles of cesium

ions and selenium ions was found. In the case of cesium ions one single peak arose from the distribution profile, whereas selenium showed two-peaks. The multiple peak system potentially indicated the different migration profiles of selenite and selenate. It is still uncertain if and how these two species influence each other in their migration behavior.

Zappey also noticed a certain discrepancy in combined experiments concerning the migration of both $^{99m}$Tc and $^{75}$Se. These inconsistencies with single-element experiments could indicate a competition between these two elements. The author appointed the discrepancies in her results to the presence of hydrogen peroxide, a strong oxidizing agent used to oxidize selenite. It still, however, poses an indication that competition between different compounds had occurred [29].

### 1.6.2. Potentially influenceable cations and oxyanions

Types of selenium species deserve special attention. It is important to do qualitative research on the migrating species before and after the experiment has been conducted. Selenite is much less mobile than selenate for example [24]. In the previous research selenite was oxidized to selenate using hydrogen peroxide as the oxidizing agent. Oxidizing with peroxide is an equilibrium process and will not result in a 100% conversion [26]. This thesis will also pay attention to qualitative analysis of the migrating species of selenium. Contrary to previous research of Zappey, selenium will not be dissolved in hydrogen peroxide.

The inner- and outer-sphere complexes formed by selenium oxyanions can also be formed by other oxyanions. Silicates, for instance, are a strong candidate as they are present in the near field and are also retained in clayey soils by the formation of inner-sphere complexes. Silicates are abundant in vitrified glass and concrete serving as barriers for HLW. Combined experiments of selenium oxyanions and silicates have been conducted in this thesis and have been compared to migration experiments with just selenium oxyanions.

### 1.6.3. Research questions

Based on results of [29] and recommendations proposed therein, we have identified two major questions to be addressed within this thesis: 1) the competition between selenite and other oxyanions, like selenate and silicate, that are expected to be present in the near-field. And 2) explaining the results that [29] found concerning the multiple peak migration pattern of selenate, which the author believes to be caused by hydrogen peroxide.

In addition to the main research questions, there are a few related issues that have also been tackled. 1) The identification of the oxidation state of selenium used in the migration experiments before and after the tests. 2) The improvement of the experimental setup. 3) The influence of sample preparation, with respect to the homogeneity of the bentonite core, by electroosmosis on the results of the migration experiments. And 4) the phase preference of bentonite for sorption of selenium species.

Based on the results of [29], competition between selenate and metasilicate, which both sorb with inner sphere complexes, is expected. The multiple peak distribution profiles in selenium migration experiments observed in [29] are believed to be caused by two migrating species of selenium. Also, optimized bentonite core preparation is likely to improve the accuracy of the results.

# 2. EXPERIMENTAL

## 2.1. An electromigration cell

Migration experiments were conducted on cesium and selenium ions traveling through bentonite. Radioactive $^{134}Cs$ and $^{75}Se$ were prepared in order to track migration paths of the corresponding elements. Due to the fact that bentonite has excellent low-permeability and high sorption properties [4], a real-life experiment on the migration behavior of radionuclides would take a long time. In order to speed up the experiment an electromigration cell, built on the principles of previous research[8, 25], was utilized (see figure 10).

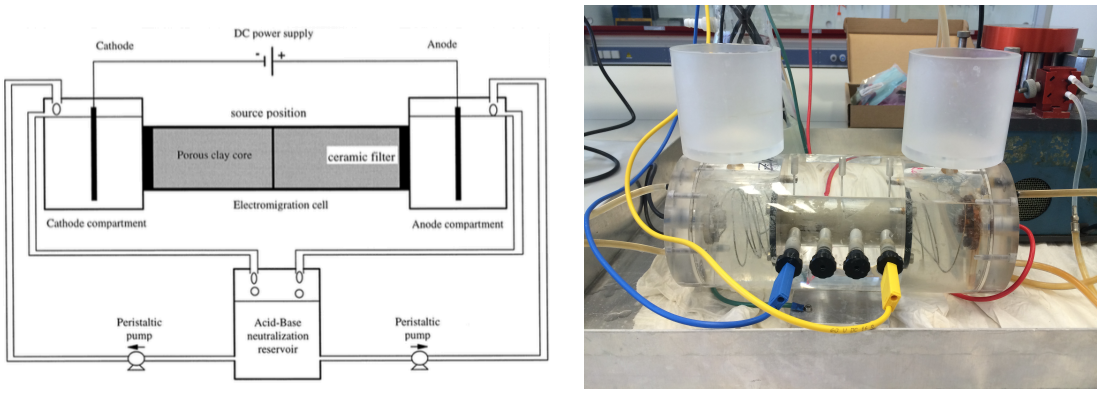


**Figure 10: Left a schematic overview of the electromigration cell[8]. Right: a picture of cell used in this thesis.**

The electromigration cell consists of a 10 cm long cylindrically shaped Plexiglas core holder, with a 3 cm diameter, in which a bentonite core sample can be placed. A 100 $cm^3$ Plexiglas electrolyte compartment resides on both ends of the sample holder. Two, 40 mm diameter, glass filters (VWR 511-0054, 40 mm diameter) seal off the sample from the electrolyte compartment. The filters allow electrolyte solution to pass through into the sample, while prohibiting bentonite from entering the electrolyte compartments. On the outer ends, both compartments were sealed by screwing on a lid. A stainless steel coil with a diameter of 1 mm was integrated in the lids, allowing the lids to serve as electrodes.

In order to regulate the electrical field over the bentonite sample, the electrolyte compartments were attached to a DC power supply (Aim TTi PLH250-P 250V 0,375A LXI). The power supply ensured a stable current through the sample. The potential through the cell and the sample could vary due to changes in electrical

resistance of the sample. In order to measure the electrical field, which, as the driving force of the migration, is one of the most important parameters, over the bentonite sample, four stainless steel electrodes were placed every 25 mm and attached to a multi meter (Agilent 34450A $5^{1/2}$ Digit Multimeter). The electrical field was monitored by Labview software. The Labview script can be found in appendix 1.

As pH is of influence to the oxidation state of the radionuclides, it was measured hourly in both compartments during the experiments. A few mL of electrolyte solution was pipetted into a 5 mL plastic vial and measured using a Metrohm 744 pH-meter. Due to electrolysis, the pH in both compartments will change in the course of the experiments. To prevent a pH gradient from occurring, the solutions from both compartments were constantly mixed in a 1,0 L mixing vial. Two peristaltic pumps (Thermo Scientific FH30) were used to pump solution in and out of the compartments and mixing vial (see figures 10, 11). The pH of Wyoming bentonite is reported in literature to be between 8 and 10 [7, 8].

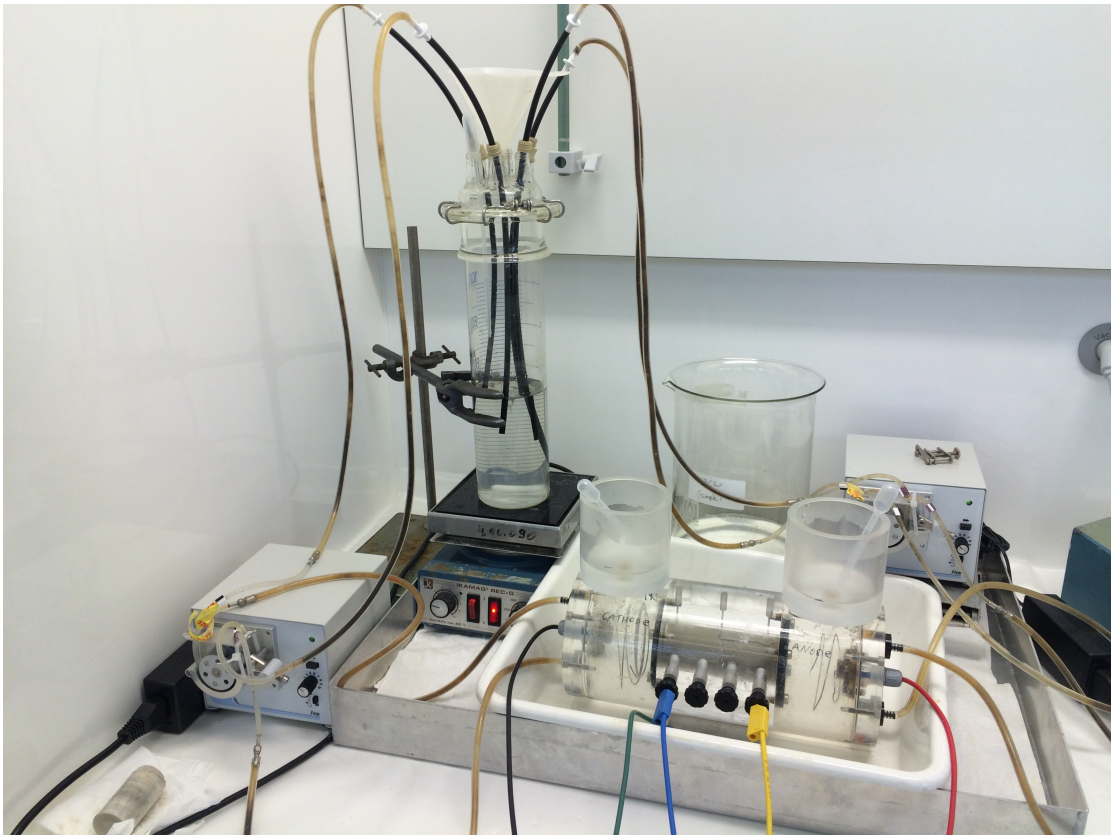

**Figure 11: Picture of experimental setup, including the electromigration cell, peristaltic pumps and mixing vial.**

Literature suggests the formation of an acid front in the saturated bentonite sample used in electromigration experiments due to the higher mobility of $H^+$ compared to $OH^-$ [30]. Because of the short duration of the experiments conducted in this thesis, the formation of an acid front can be dismissed.

A second parameter that influences the speciation of the radionuclides is the reduction potential, or $E_h$. Because a relatively large potential is applied over the cell, $E_h$ was expected to be high and measurements were not needed. pH on the other hand can vary outside of the perimeters of the selenium species of interest (see section 1.5.2.) and is thus essential to regulate.

The experimental setup described in this paragraph and the sample preparation technique described in paragraph 2.3.3. can also be utilized with alternative materials e.g. cement in the CEBAMA project.

## 2.2. Electrokinetic transport phenomena

### 2.2.1. An overview of the relevant electrokinetic transport phenomena

The physics of electromigration is a little more complex than regular, electric field free, migration. The combinations of electrical and hydraulic flows in electrolytic water can be held accountable for a couple of electrokinetic phenomena. In this thesis electrophoresis and electroosmosis are of interest (see figure 12). These two phenomena result from the force that an external electric field exerts on the sample, the migrating ion and surrounding ions [7, 8].

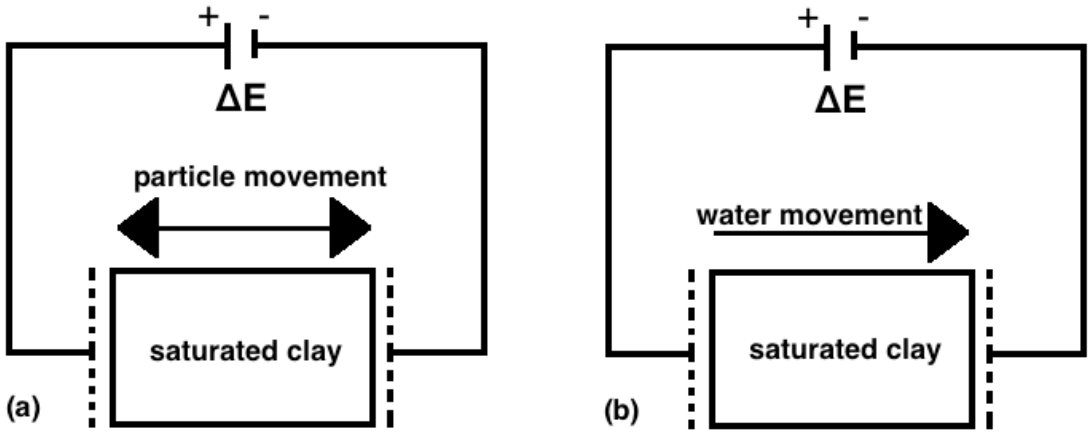


**Figure 12: Schematic overview of electrokinetic transportphenomena. a) Electrophoresis. b) Electroosmosis.**

Electrophoresis (figure 12a) is the process of which charged particles move through a medium under influence of an electrical field. The particles are electrostatically attracted to either the anode or the cathode, depending on the nature of their charge.

Electroosmosis (figure 12b) is the effect of a viscous drag that ions exert on the water molecules around them. In a porous medium that consists of negatively charged particles, like clay minerals, an accumulation of positively charged ions from the soil solution occurs around these clay minerals. These positively charged species are attracted by the cathode and drag water molecules with them. The viscous drag results in a net flow of water towards the cathode [7, 30].

Both electrokinetic phenomena have an effect on the radioactively labeled ion. In the case of cations, both phenomena push the cation towards the cathode, whereas an anion is attracted towards the anode, but pulled back by electroosmosis. The velocities at which the ions travel can be expressed as vectors and are both proportional to the strength of the electrical field. As seen in figure 13, the measured velocity in the experiments is a sum of these vectors [8].

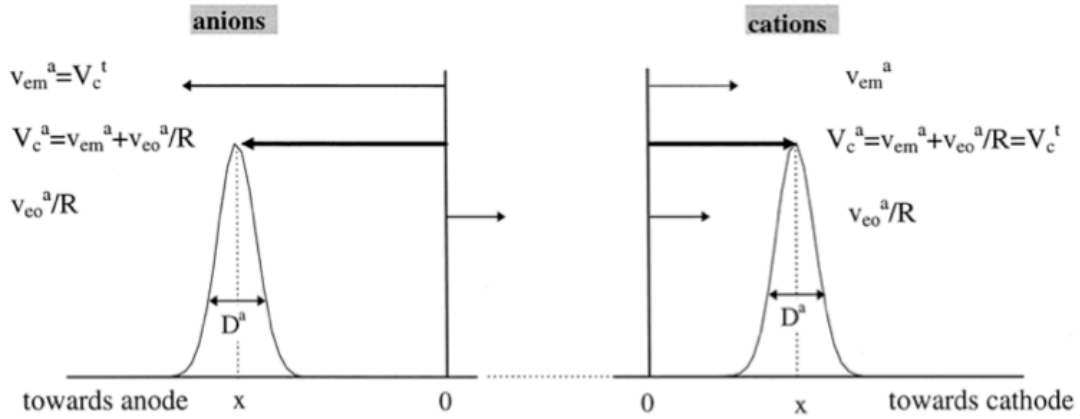


**Figure 13: Schematic overview of the sum of velocities that make up the total convection velocity. $V_{eo}$ is the velocity contributed by electroosmosis. $V_c^t$ is the total convection velocity. $V_{em}$ is the velocity contributed by electromigration (electrophoresis). $V_c^a$ is the apparent convection velocity. R is the retardation factor and $D^a$ is the dispersion coefficient.**

The transport of radionuclides in a clayey medium that has been subjected to an electrical field is mathematically described by a one-dimensional advection-dispersion equation based on Fick's second law. A full model was given by Maes

et al. [8, 31]. For the purpose of this thesis only the relevant parts of the equation will be explained.

### 2.2.2. Relating ion velocity to the molecular diffusion coefficient

Newton's second law describes the velocity at which an ion travels to its counter-charged electrode. A driving force, in this case the Coulomb force, pushes the ion towards the electrode. A drag force called Stokes drag retards the ion. The resulting equation is given by equation 1:

$$m\frac{dv}{dt} = qE - 6\pi\mu r v \tag{1}$$

In equation 1 the Coulomb force is expressed by the charge of the particle, q [-], and the electric field by E [V/m]. Stoke's drag is expressed by the radius of the particle r [m], the velocity of the particle $v$ [m/s] and the viscosity of the fluid μ [Ns/m$^2$]. If there is no acceleration, equation 1 can be written in terms of velocity as the "drift speed equation" (equation 2):

$$v = \frac{q}{6\pi\mu r}E \tag{2}$$

As seen in equation 2 and mentioned in section 2.2.1., the speed at which a charged ion moves through a medium is proportional to the electrical field applied over the medium. The constant that describes this proportionality is called the ionic mobility, $\mu_e$ [m$^2$/sV].

$$\mu_e = \frac{v}{E} = \frac{q}{6\pi\mu r} \tag{3}$$

Finally, the Einstein relation can be used to relate the molecular diffusion coefficient with the electrical field [8, 32]:

$$D_m = \frac{\mu_e K_b T}{Ze} \tag{4}$$

In which $D_m$ stands for the molecular diffusion coefficient [m$^2$/s], $K_b$ is the Boltzmann constant [J/K], T is the temperature [K], Z is the valence of the particle [-] and $e$ is the charge of an electron [C].

### 2.2.3. The apparent dispersion-convection equation

The transport of chemical species is given by the general dispersion-convection equation [8], which is a variation on Fick's second law:

$$\frac{dC}{dt} = D\frac{d^2C}{dx^2} - V_c\frac{dC}{dx} \tag{5}$$

In which the first term is the dispersion term, with D being the dispersion coefficient [$m^2/s$], and the second term is the convection term, with $V_c$ being the convection velocity [m/s]. As mentioned in section 2.2.1., the convection velocity is built up out of two vectors, both dependent on the electrical gradient: the electromigration velocity, $\nu_{em}$, and the electroosmotic velocity, $\nu_{eo}$.

$$V_c = \nu_{em} + \nu_{eo} \tag{6}$$

Because of the porosity of bentonite, equation 5 has to be adapted for tortuosity and retardation. Retardation meaning any process (sorption, ion-exchange, etc.) that can prevent an ion from migrating. Tortuosity, $\tau$ [-], is the ratio between the actual distance of a diffusion path, $x$ [m], and the experimentally measured distance from end to end, $z$ [m]. The value of $\tau$ is always greater than 1 and the relationship is given by equation 7:

$$\tau = \frac{x}{z} \tag{7}$$

The adapted version of equation 5 results in equation 8:

$$\frac{dC}{dt} = \frac{D}{R\tau^2}\frac{d^2C}{dz^2} - \frac{V_c}{R\tau^2}\frac{dC}{dz} \tag{8}$$

With R being the retardation factor [-]. $\frac{D}{R\tau^2}$ can be substituted by the apparent dispersion coefficient, $D^a$, and $\frac{V_c}{R\tau^2}$ can be substituted by the apparent convection velocity, $V_c^a$, giving the final apparent dispersion-convection equation:

$$\frac{dC}{dt} = D^a\frac{d^2C}{dx^2} - V_c^a\frac{dC}{dx} \tag{9}$$

### 2.2.4. Deriving the apparent molecular diffusion coefficient

The hydrodispersion relationship gives the general relationship between the apparent dispersion coefficient and the apparent molecular diffusion coefficient.

$$D^a = D_m^a + \alpha V_c^t \quad (10)$$

$D_m^a$ is the apparent molecular diffusion coefficient [m²/s], α is the dispersion length [m], and $V_c^t$ the total apparent convection velocity. It is important to notice that the total apparent convection velocity ($V_c^t$) is not always the same as the apparent convection velocity ($V_c^a$). As shown in figure 13, the total apparent convection velocity is a sum of vectors and it is the velocity that will cause dispersion.

$$V_c^t = v_{em}^a + \frac{v_{eo}^a}{R} = V_c^a, \qquad \text{in case of cations} \quad (11)$$

$$V_c^t = v_{em}^a = V_c^a + \frac{v_{eo}^a}{R}, \qquad \text{in case of anions} \quad (12)$$

A Matlab script (see appendix 2) has been utilized to fit the experimental data (distribution profiles) to the calculated data, in order to obtain the apparent dispersion coefficient ($D^a$). Matlab used a solution of equation 9 to calculate the apparent dispersion coefficient:

$$C(x,t) = \frac{Q_0}{2S\sqrt{\pi D^a t}} exp\left(-\frac{(x-V_c^a t)^2}{4D^a t}\right) \quad (13)$$

Where C is the concentration of the species, $Q_0$ is the initial activity [Bq], S is the cross-section of the sample and t is the experimental time [s].

With $D^a$ and $V_c^t$ known, results from multiple experiments were plotted to obtain a value for the apparent molecular diffusion coefficient. This was done by extrapolating the trend line of several data points.

## 2.3. Experimental procedures

This section covers the work done in the lab. For detailed experimental procedures see appendix 3, 4 and 5. Section 2.3.1., 2.3.2. and 2.3.3. discuss the preparation of synthetic boom clay water, the radioisotopes and a homogeneous bentonite core. Section 2.3.4. covers the actual migration experiment. Finally, section 2.3.5. and 2.3.6. are about experiments concerning a qualitative analysis of the migration species in the case of selenium and the analysis of the preference of selenium ions for the sorption on the solid clay phase or remaining in the liquid pore-water phase.

### 2.3.1. Preparation of synthetic boom clay water

The electrolyte used in the electrolyte compartments should resemble the pore water in real-life conditions. Boom clay pore water (BCW) mostly consists of sodiumhydrogencarbonate ($NaHCO_3$) and a few small fractions of other components. A detailed recipe for synthetic boom clay water (SBCW) made by SCK•CEN is given in appendix 6 [33]. For the purpose of this thesis it was chosen to use a simplified SBCW consisting only of its main component ($NaHCO_3$). A 15 mM $NaHCO_3$ (pH=8.86) solution was used as electrolyte.

### 2.3.2. Isotope preparation

Due to the long half-life time of $^{137}Cs$ and $^{135}Cs$, the γ-emitter $^{134}Cs$ with a half-life time of approximately two years is used in this thesis. Cesium has a 100% natural occurrence of the stable $^{133}Cs$ isotope. To produce 1 MBq of $^{134}Cs$, 10 mg of CsCl was irradiated for 240 minutes at the RID (Reactor Institute Delft) with a mixture of:

- an apithermal neutron flux of $4.45*10^{14}$ [$1/sm^2$]
- a thermal neutron flux of $4.59*10^{16}$ [$1/sm^2$]
- a fast thermal flux of $3.24*10^{15}$ [$1/sm^2$]

After irradiation, the sample was cooled for three days to let active by products decay. The reaction, involving neutron capture, is given below:

$$^{133}_{55}Cs + ^{1}_{0}n \rightarrow ^{134}_{55}Cs + \gamma$$

$^{134}CsCl$ was dissolved in 0.1M NaOH (pH = 13) in order to preserve the alkaline nature of BCW.

Because of the very long half-life time of $^{79}Se$, the γ-emitter $^{75}Se$ with a half-life time of approximately one hundred and twenty days is used in this thesis. To produce 1 MBq of $^{75}Se$, 25 mg of $^{74}SeO_2$ (natural selenium mixture with <1% $^{74}Se$ content) was irradiated for 600 minutes at the RID. Under the applied condition only the yield of $^{75}Se$ is significant. The sample was irradiated with a mixture of:

- an apithermal neutron flux of $4.45*10^{14}$ [$1/sm^2$]
- a thermal neutron flux of $4.59*10^{16}$ [$1/sm^2$]
- a fast thermal flux of $3.24*10^{15}$ [$1/sm^2$]

After irradiation, the sample was cooled for three days to let active by products decay. The reaction, involving neutron capture, is given below:

$$^{74}_{34}Se + ^{1}_{0}n \rightarrow ^{75}_{34}Se + \gamma$$

Irradiated $SeO_2$ was dissolved in 0.1M NaOH (pH = 13) in order to preserve the alkaline nature of BCW. By dissolving $SeO_2$, selenite was formed in the following reaction [26]:

$$SeO_2 + 2NaOH \rightarrow Na_2SeO_3 + H_2O$$

### 2.3.3. Sample preparation

It is of great importance that saturation and molecular composition of the bentonite samples used in migration experiments closely resemble the real-life conditions 200 meters below the biosphere. They have to be completely saturated with pore water, have the same molecular composition as bentonite used in real-life and if possible anaerobic. Three methods have been identified and tested.

First, the quickest method for preparing the core is by pre-mixing equal amounts (weight) of clay and water and manually kneading it thoroughly to get a sample as homogenous as possible. The clay was casted into two 5 cm cylinders with a 3 cm diameter. This method is quick (20 minutes), but allows for a lot of insaturations as it is near impossible to insert the two 5 cm cylindrical clay samples into the sample holder without creating pores or changing its density.

Second, the sample can be prepared using electroosmotic water flow. Two hollow polycarbonate vials (see figure 14) with an inner diameter of 2.8 cm were inserted into the cell's sample holder and then filled with bentonite powder. Every 5 mm a drop of SBCW was added to ensure conductivity at the start of the sample preparation. To account for expansion of the sample, that

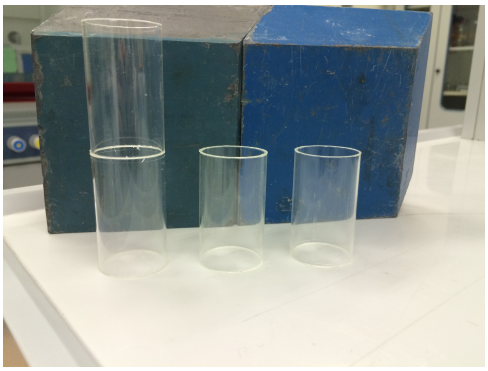

**Figure 14: Polycarbonate vials used for clay core preparation.**

can crack the glass filters, only 9.5 cm of the sample holder was filled with powder. Both electrolyte compartments were then filled with SBCW and 15 mA was applied over the cell. Electroosmosis forced water from the anode to the cathode, saturating the sample on its way. When the potential over the core (measured with the multimeter) stabilized, saturation was complete (see figure 15). Homogeneity of the core was preserved inside the polycarbonate vials, allowing the core to be removed from the sample holder and placed back later for active experiments. This method takes about 24 hours for complete saturation. Iron ions from the bentonite powder are attracted to the anode. Saturating the core for longer than 24 hours might influence the composition of the core significantly as the formation of FeOH was seen in the anode compartment during longer core preparations.

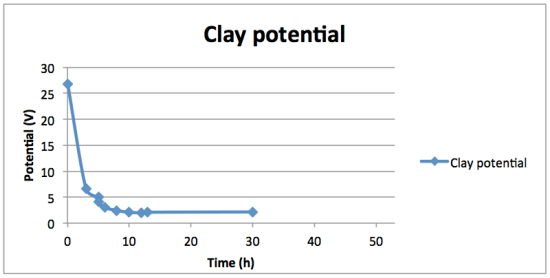


**Figure 15: Graph shows decreasing resistance (and increasing saturization) of the clay core.**

Last, 10 cm Plexiglas tubes with a 3 cm diameter were available. The same 5 cm polycarbonate vials were inserted into the tube, filled with bentonite powder and sealed with a porous filter. They were then left to saturate in SBCW for approximately 2 months. This method takes a long time, but ensures preservation of homogeneity and no changes in the bentonite's molecular composition.

In this thesis the second method was preferred, due to the relatively short preparation time and preservation of homogeneity of the core. All methods can be done under anaerobic conditions. However, it was chosen to work under aerobic conditions as the bentonite powder was bought already oxidized. It was assumed that competition between selenate and metasilicate could be seen regardless of aerobic or anaerobic conditions.

Metasilicate solution, used in three combined experiments, was made by dissolving 1.826 mg of $Na_2SiO_3 * 5H_2O$ in 200 µL of SBCW (equal molarity as Se solution).

### 2.3.4. Electromigration experiments

The bentonite core pieces, still in their 5 cm polycarbonate vials, were placed in the sample holder. After placing the first 5 cm back in the sample holder, some filter paper was put in the middle of the sample holder. The filter paper was wetted with SBCW and spotted with active solution (50 µL). Between 150 and 250 kBq of activity was spotted in each experiment. The second 5 cm of saturated core was placed in the sample holder and the sample holder was sealed with the glass filters. After filling both compartments with SBCW the experiment was conducted.

The potential over the clay core was monitored by LabView software. pH was also measured hourly in order to make adjustments if needed to stay within the 8-10 pH range of natural BCW.

The electrical current over the cell was set to a constant value. The potential over the cell and the clay core varied with changing electrical resistance of the clay. The average electrical field was noted for further calculations.

After an experiment, the polycarbonate vials, with the clay core still in them, were pushed out of the electromigration cell. The core was left to dry for two hours. During this time the clay shrunk slightly, which made it easier to remove from the vials. After the clay was removed from the vials, it was cut into 5 mm pieces with a thin spatula. Each piece was put into a 50 mL plastic vial, whereafter 40 mL of milli-q water was added. The vials were shaken on a rotator overnight.

After being shaken, 10 mL of each vial was moved into glass scintillation vials suitable for a Wizard 2480 automatic gamma counter (Wallace). The vials were run through the gamma detector, measuring every vial for 600 seconds.

The data from the Wallace detector was exported into Origin and Matlab, resulting in a distribution profile and a value for $D^a$ and $V_c^t$.

### 2.3.5. Selenite reduction

Two experiments were conducted for the qualitative analysis of the oxidation state of selenium. One to determine the state of selenium before the migration experiment and the other to determine the state after it had run through the migration cell and had been subjected to an electric field.

Selenite was formed by dissolving 25 mg of $SeO_2$ in 2 mL of 0.1 M NaOH in a 15 mL plastic vial. A surplus of thiourea was added to the solution and it was manually shaken for 60 seconds. After the vial turned red, indicating elemental selenium (figure 16), the vial was rotated at 3900 RPM in a Jouan CR4i centrifuge. The supernatant was taken and transferred to a clean 15 mL plastic vial. The process of adding thiourea, rotating and removing the supernatant was repeated until the solution didn't turn red anymore after adding thiourea. This indicated that all Se(IV) had been reduced. Inductive coupled plasma mass spectrometry (ICP) (PerkinElmer Optima 5300 DV) analysis was conducted on the clear sample in order to determine the concentration of selenium left in solution. As all Se(IV) should be reduced, any selenium left is Se(VI), which is much harder to reduce [25, 34].

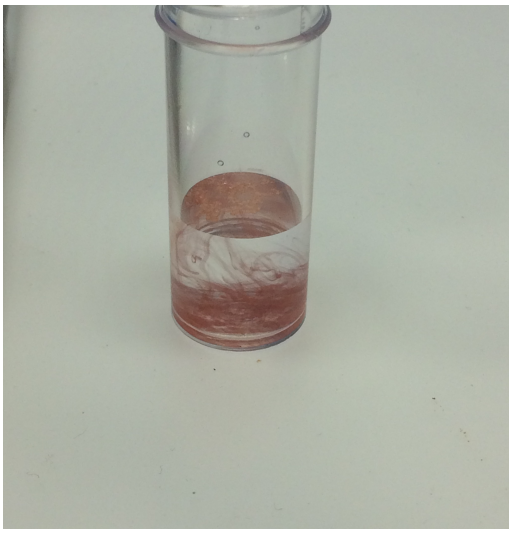

**Figure 16: Reduction of $SeO_3^{2-}$ to $Se^0$ by thiourea can be seen by the reddish color of elemental selenium.**

To determine the oxidation state(s) of selenium after the migration experiment, 25 mg of $SeO_2$ was dissolved in 200 µL 0.1 M NaOH (measured pH = 12.75). After preparing a clay core, 50 µL of solution was spiked in the middle of the core and a non-active migration experiment was conducted for 3.5 hours at 15 mA. After

the experimental time had passed, the core was sliced in slices of 5 mm and put in 50 mL vials. The vials were filled with 45 mL milli-q water and shaken for 48 hours. After two days, the vials were rotated at 3900 RPM for 20 minutes each. 5 mL of 0.1 M NaOH (measured pH = 12.75) was added to facilitate phase separation of the suspension. Each vial was then rotated at 3900 RPM for 20 minutes again. The clear supernatant was then removed and transferred into 15 mL plastic vials. The same cycle as in the previous experiment of adding thiourea, rotating and transferring supernatant was then applied. The solution was measured for selenium concentration with ICP.

After ICP-analysis, one of the solutions that had selenium in it was dried in a glass beaker on a hot plate for five hours. 18.6 mg of solid was recrystallized for XRD analysis.

### 2.3.6. Phase separation of dispersed clay

In order to identify if selenium species were sorbed to the solid phase or resided in the mobile "pore" water phase, a phase separation was preformed on the clay samples of one migration experiment. After being shaken overnight on a rotator, 5 mL of NaOH (pH = 13.01) was added to each vial. The vials were then centrifuged for 20 min at 3900 RPM. The result of the centrifugation was a three-phase system (see figure 17). The phases consist of a solid precipitant, a gel and a clear liquid phase. Each phase was analyzed by the γ-detector to determine the preference of selenium species for each phase.

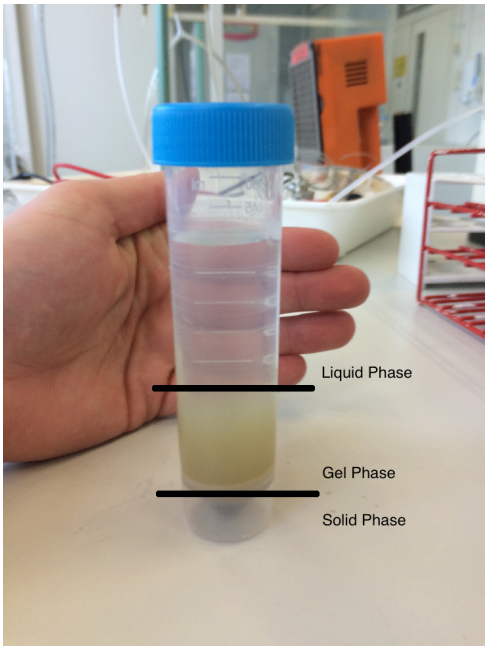


**Figure 17: Photo of the three phase system after adding NaOH and rotating. The dark bottom system is the solid phase, the light brown phase is the middle is a gel, the top phase is clear and liquid.**

# 3. RESULTS AND DISCUSSION

## 3.1. Bentonite core preparation and mineralogical analysis

### 3.1.1. Core preparation

Many trial experiments were conducted in order to create the method of core preparation explained in section 2.3.3. The aim was to create a technique, using electroosmosis, that would take a relatively short amount of time (<30 hr) and maintain homogeneity of the bentonite core. Experimental conditions and results are listed in table 1. Detailed observations of all core preparation experiments can be found in appendix 7.

**Table 1: Experimental conditions under which core preparation experiments were conducted.**

| Exp. code | Time [hr] | Current [mA] | pH | Polycar-bonate vial? | Comments |
|---|---|---|---|---|---|
| **Core-1** | 100 | 60 | 7.5 - 8.0 | no | Cracked filter, Fe-precipitation |
| **Core-2** | 52 | 25.2 | 4.0 - 13 | no | Pump failure |
| **Core-3** | 53 | 15 | 8.2 - 10 | yes | |
| **Core-4** | 25.5 | 15 | 8.0 - 9.5 | yes | Sample holder filled 95% |

Using polycarbonate vials to encapsulate the saturating core, ensured the preservation of homogeneity. By wetting the bentonite powder with SBCW when filling the polycarbonate vials, initial conductivity in the core is accomplished. Figure 18 shows the difference between barely wetting the powder (core-3) and heavily wetting the powder (core 4). The final experiment had a much lower initial electrical resistance and was therefore saturated in approximately one day. The techniques used in experiment core-4 were chosen for the electromigration experiments in this thesis.

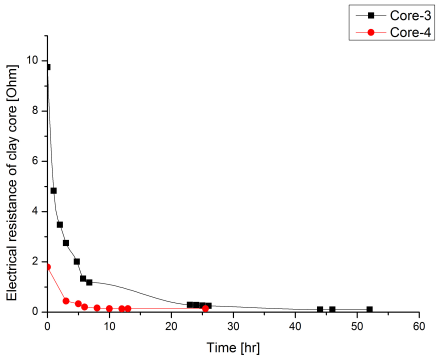


**Figure 18: Experimental results of the electrical resistance of the saturating bentonite core developing over time.**

### 3.1.2. Mineralogical analysis of Wyoming bentonite

Mineral composition of Wyoming bentonite given by [36] (table 2) was compared with XRD analysis on the Wyoming bentonite (Cebogel Wyoming API, Cebo Holland B.V.) used in this thesis. Two samples of bentonite powder were analyzed. The first sample consisted of untouched powder from the manufacturer. The second sample was heated for 12 hours at 800 °C before analysis. Figure 19 shows a mostly amorphous pattern, which is due to the high montmorillonite content of bentonite. Quartz ($SiO_2$), calcite ($CaCO_3$) and albite ($Na(Si_3Al)O_8$) were identified as crystaline components. These minerals and the presence of calcium are consistent with the data from [36].

Table 2: Mineral content of Wyoming bentonite by [36].

| Component | wt-% |
|---|---|
| Montmorillonite | 87 |
| Mica | 4 |
| Albite | 3 |
| Quartz | 3 |
| Cristobalite | 2 |
| $Na^+$ | 72 |
| $Ca^{2+}$ | 18 |
| $Mg^{2+}$ | 8 |
| $K^+$ | 2 |

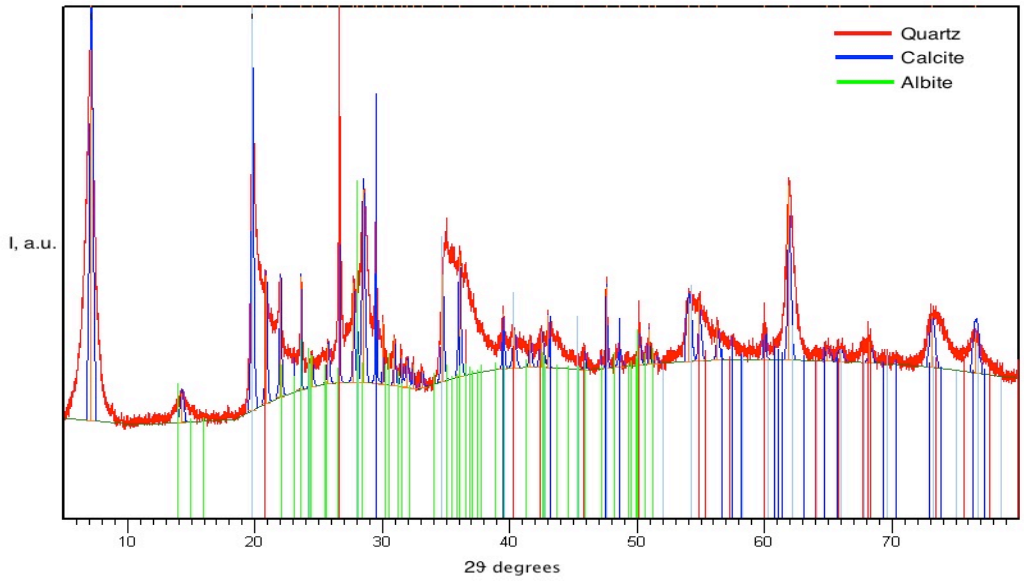


Figure 19: XRD spectrum for Wyoming bentonite from the manufacturer.

After heating calcite had decomposed, as its decomposition temperature is 615 °C [35]. Crystaline haematite ($Fe_2O_3$) was detected in the heated sample, indicating the presence of iron, which could also be seen by eye due to the red color of the heated powder.

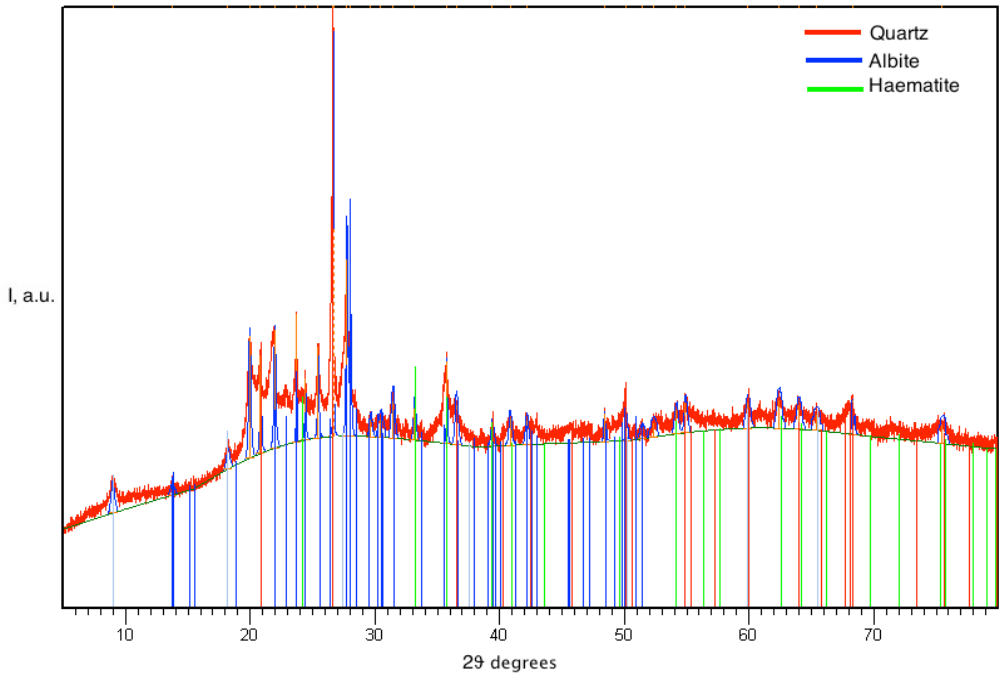


Figure 20: XRD spectrum for Wyoming bentonite after heating to 800 °C.

## 3.2. Cesium

Two experiments with cesium were conducted with the goal of testing the improved electromigration cell. The experimental conditions were chosen to resemble Cs-7 described in [29] due to its relatively short experimental time. Even though experimental time was considerably lower than with the core preparation, the first experiment failed due to a cracked filter in the anode compartment. Negatively charged clay particles, attracted towards the anode, exerted too much pressure on the filter. Future experiments were conducted at a lower current and electrical field.

By fitting the experimental distribution profile (figure 21) in Matlab, the dispersion coefficient and apparent velocity were calculated. The results were compared with Zappey's distribution profile (figure 22) and values for the dispersion coefficient and the apparent velocity. Table 3 lists the results of the calculations in Matlab.

Table 3: Experimental conditions and results of conducted active cesium experiments of this thesis and Zappey's [29].

| Experimental code | Time [hr] | Electric field [V/m] | Current [mA] | pH | $D^a$[m²/s] | $V_c^t[m/s]$ |
|---|---|---|---|---|---|---|
| Cs-1 Carter | 7 | 58 | 40 | 9.1 | | |
| Cs-2 Carter | 6.5 | 41 | 30.1 | 8.9 | 5.75E-10 | 1.07E-07 |
| Cs-7 Zappey | 6.5 | 46 | 25 | 9.3 | 1.08E-08 | 2.56E-08 |

The values found for the dispersion coefficient and the total convection velocity are not a reliable measure for comparison though, as they are dependent on experimental time, current, pH, electrical field and saturation of the clay core. Maintaining constant values for these parameters is near impossible with the utilized set-up. The values do show that approximately the same conditions were created as in Zappey's experiment. Because only one experiment was conducted, the apparent molecular diffusion coefficient was not determined.

Of bigger relevance is the comparison of both distribution profiles (figures 21 and 22). The experimental profile looks very similar to Zappey's in shape and distance and therefore confirms that her results can be reproduced with the improved electromigration cell and the method of clay core preparation.

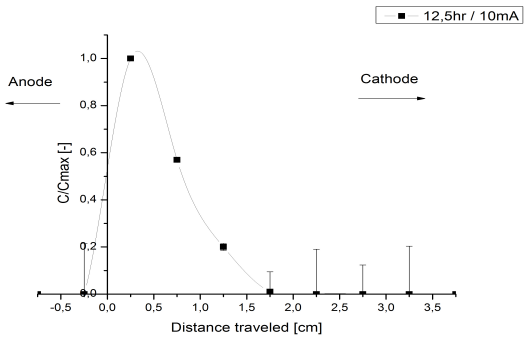


Figure 21: Distribution profile of Cs-2.

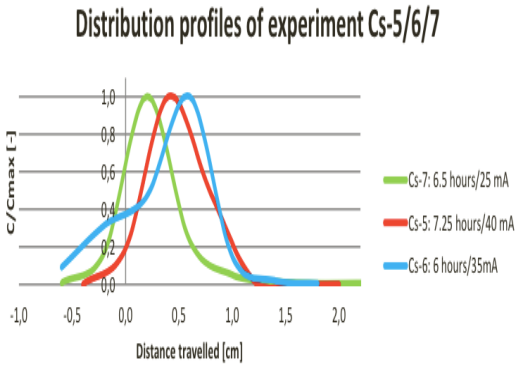


Figure 22: Distribution profiles of Zappey 's cesium experiments [29].

## 3.3. Selenium

### 3.3.1. Qualitative analysis of selenium species

Two experiments were conducted in order to determine which species of selenium is used in the migration experiment and to determine if there is a change in oxidation state during the migration process.

ICP analysis of the first experiment (see section 2.3.5) showed no presence of selenium, indicating that all selenium present before adding thiourea as a reducing agent, was in the selenite species.

The second ICP analysis was done after the selenite was subjected to the electromigration process. This time selenium was measured in solution, after reducing selenite, indicating the presence of selenate. A distribution profile, similar to the distribution profiles found in active migration experiments (see section 3.3.2.), was found. Figure 23 shows the distribution of selenate after 3.5 hours of migration under 15.0 mA. Most of the tracer remained at the center of the sample but it can clearly be seen that a negatively charged, non-reduced selenium species has migrated slightly towards the anode. As all of the selenite was reduced to elemental selenium, the species shown in figure 23 must be selenate.

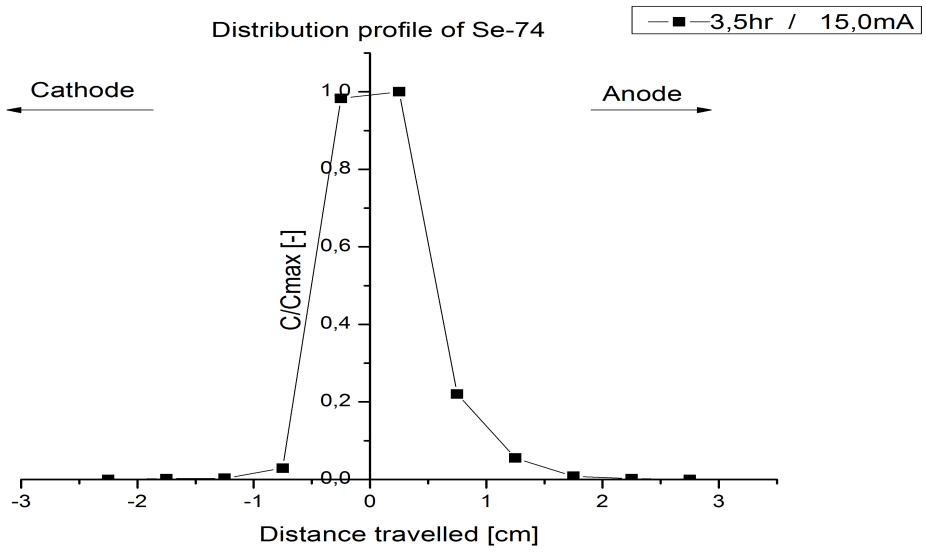


**Figure 23: Distribution profile of inactive selenate obtained by ICP analysis.**

It can be concluded that the species that selenium exists in before exposing it to an electrical field is solely selenite. This is in agreement with literature stating the reaction of $SeO_2$ with a NaOH solution [26] and the negligible oxidation of selenite [25]. The electric field, in the company of water present in bentonite, induces the oxidation of selenite during migration. This means there are two species of selenium during the experiment. The scheme of oxidation reaction is given below [26]:

$$Na_2SeO_3 + H_2O \xrightarrow{eletricity} H_2 + Na_2SeO_4$$

XRD analysis of recrystallized solid showed mostly thiourea, which was added in surplus. No selenium compounds were identified.

### 3.3.2. Migration experiments

Two experiments were conducted with $^{75}Se$ tracer. In both experiments, Se-1 and Se-2, selenium was spotted in the selenite form and partially oxidized to selenate in the course of the migration process in accordance with observations shown in section 3.3.1. The results and experimental conditions are listed in table 4.

**Table 4: Experimental conditions and results of conducted active selenium experiments.**

| Experimental code | Time [hr] | Electric field [V/m] | Current [mA] | pH | $D^a$[m²/s] | $V_c^t[m/s]$ |
|---|---|---|---|---|---|---|
| **Se-1** | 12.5 | 14 | 10 | 9.1 | 5.95E-10 | 1.00E-7 |
| **Se-2** | 17 | 16 | 10 | 8.5 | 8.95E-10 | 2.04E-7 |

Both experiments were conducted at a low current, and thus low electrical field. Experimental time was extended in order to ensure enough migration to be measurable and to prevent most of the tracer from remaining at the center. Distribution profiles of Se-1 and Se-2 are shown in figures 24 and 25.

Both distribution profiles show two peaks on the anode side of the center. The peaks are caused by the two independently migrating species of selenium: selenite and selenate. The most right peaks in both distribution profiles are assigned to the mobile selenate, whereas the left peaks are appointed to the easier adsorbed selenite. The selenite peak in experiment Se-1 (figure 24) is

larger than the selenate peak, whereas in experiment Se-2 (figure 25) this is vice versa. Longer experimental time ensures for more immobile selenite to be oxidized to mobile selenate. A rough estimation based on the data from Se-1 and Se-2 suggests that about half of the selenite is reduced to selenate in 17 hours. The tail on the cathode side of the center can be assigned to selenium ions that are dragged towards the cathode by electroosmosis.

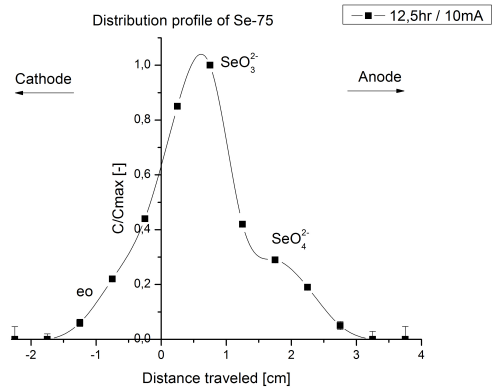


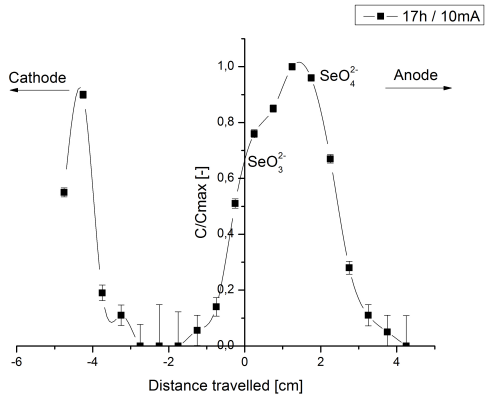


**Figures 24 (left) and 25 (right): Distribution profiles of Se-1 (left) and Se-2 (right). The peak on the far right is attributed to mobile selenate. The center peak to immobile selenite and the tail on the cathode side to electroosmotic drag. Figure 25 shows a sharp peak towards the far left. It is believed to be caused by positively charged colloids dragging activity towards the cathode or by contamination.**

Figure 25 also shows an intense peak on the cathode end of the profile. The peak might be caused by positive of neutral colloid particles that trap selenium and drag it towards the cathode. However, there is no explanation for colloid drag being present in experiment Se-2 and not in experiment Se-1. Even though great caution was taken while working with the sample, contamination should not be ruled out as the source of this peak.

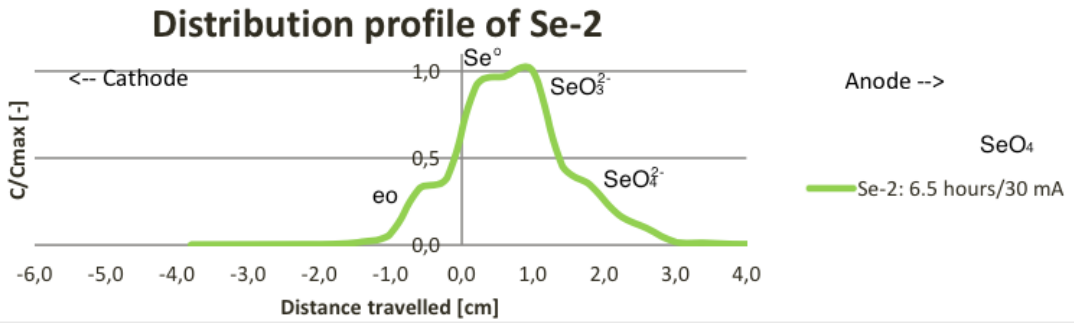


**Figure 26: Distribution profile obtained by Zappey. The experiment was conducted for 6.5 hours under 30 mA. The electric field was 47 [V/m]. The peaks were assigned by subjecting it to results found in this thesis.**

The multiple-peak distribution profile (figure 26) found by Zappey can be explained by the simultaneous migration of selenite and selenate, induced by an electric field. Section 3.4. elaborates further on the assignment of different peaks.

The apparent molecular diffusion coefficient in bentonite found for selenate was $3*10^{-10}$ [$m^2/s$] (see figure 27), which is according to literature [17] ($3.2*10^{-11}$ [$m^2/s$], and Zappey [29] ($1.0*10^{-10}$ [$m^2/s$]). The new method for preparing the bentonite clay core in polycarbonate vials seems to have little influence on the experimental results.

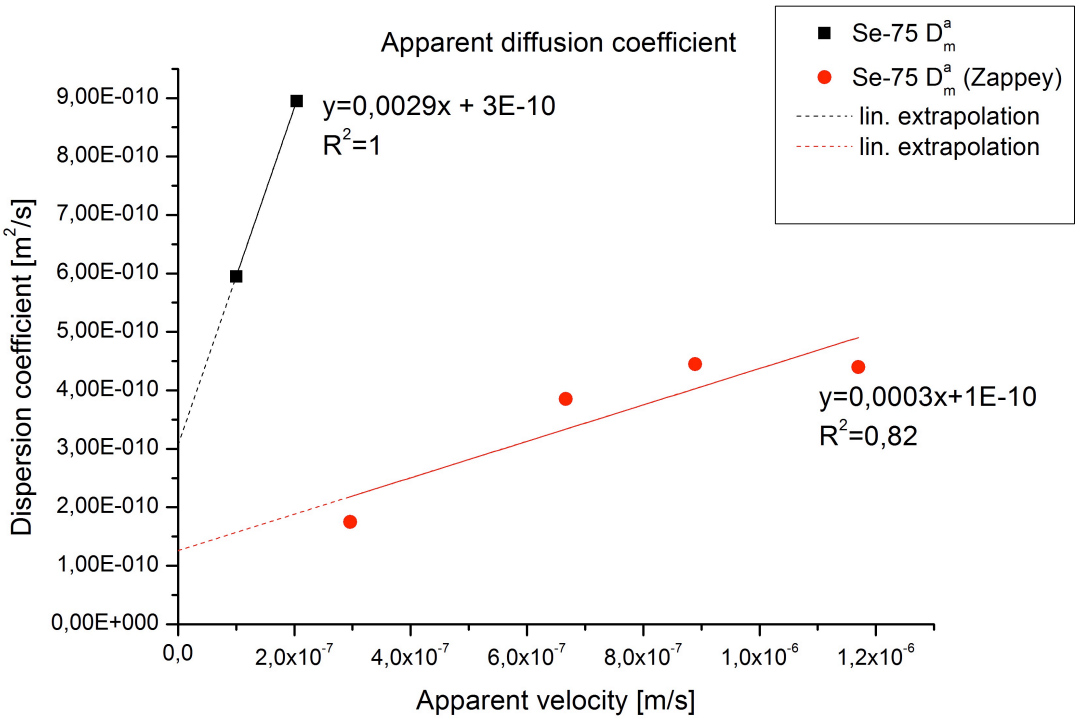


**Figure 27: Apperent molecular diffusion coeffecient obtained during the experiment with selenium in this thesis and Zappey's [29].**

### 3.3.3. Analysis of phase preference for sorption

In order to determine the preferred medium selenium species reside in, one experiment was conducted separating the solid, gel and liquid phase in bentonite. Figure 28 shows the distribution profile of Se-1 broken down into three profiles. The shape of the three profiles resembles the overall distribution profile. There is a major difference in intensity between the solid phase and the gel and liquid phases, indicating that selenium ions were not adsorbed to the

solid phase but remained in the pore water. This is in agreement with the data on selenate being very mobile and not easily adsorbed.

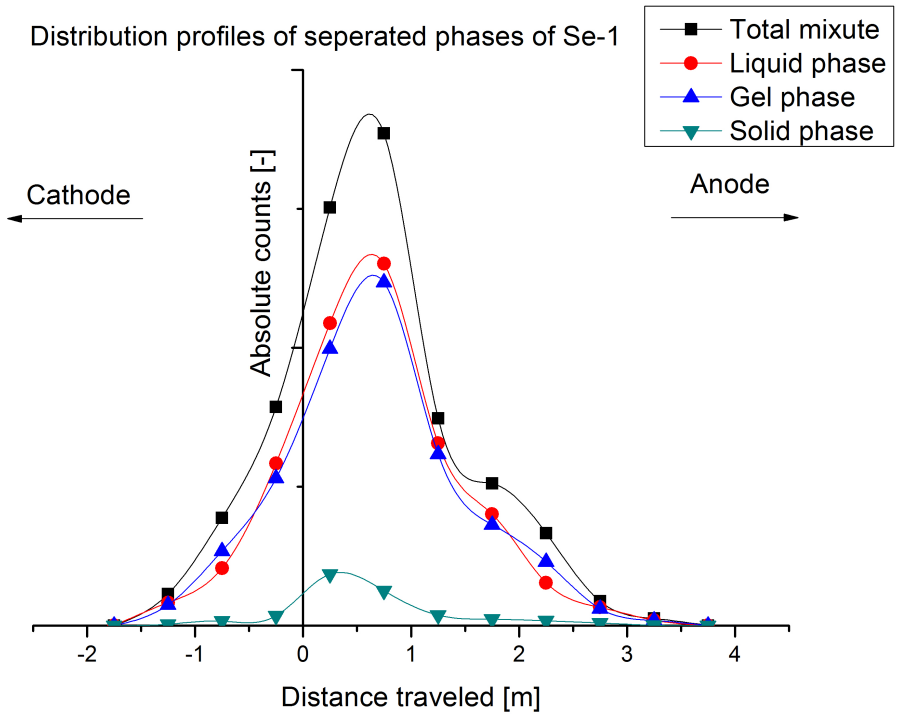


**Figure 28: Distribution profiles of phase separated selenium experiment. Only a small fraction of the selenium species reside in the solid phase.**

## 3.4. Combined experiments between Selenate and metasilicate

As stated in section 1.6.2. the potential influence of competition between selenate and other oxyanions has been investigated. Three combined experiments were conducted with active selenium and non-active metasilicate. Again, the initial species of selenium was selenite and is oxidized to selenate during the migration process. The results are shown in table 5.

**Table 5: Experimental conditions and results of conducted active selenium and non-active metasilicate experiments.**

| Experimental code | Time [hr] | Electric field [V/m] | Current [mA] | pH | $D^a$[m²/s] | $V_c^t[m/s]$ |
|---|---|---|---|---|---|---|
| $Se/SiO_3$ - 1 | 6.5 | 16.2 | 10 | 8.5 | 5.15E-10 | 1.07E-07 |
| $Se/SiO_3$ - 2 | 9.5 | 14.0 | 10 | 8.7 | 1.18E-09 | 4.53E-07 |
| $Se/SiO_3$ - 3 | 12.5 | 12.5 | 10 | 8.8 | 7.75E-10 | 2.33E-07 |

Figures 29 and 30 show the distribution profiles of Se/SiO3-1 and Se/SiO3-3. The last figure shows the colloid-drag activity tail near the cathode also seen in Se-2 (see section 3.3.2.).

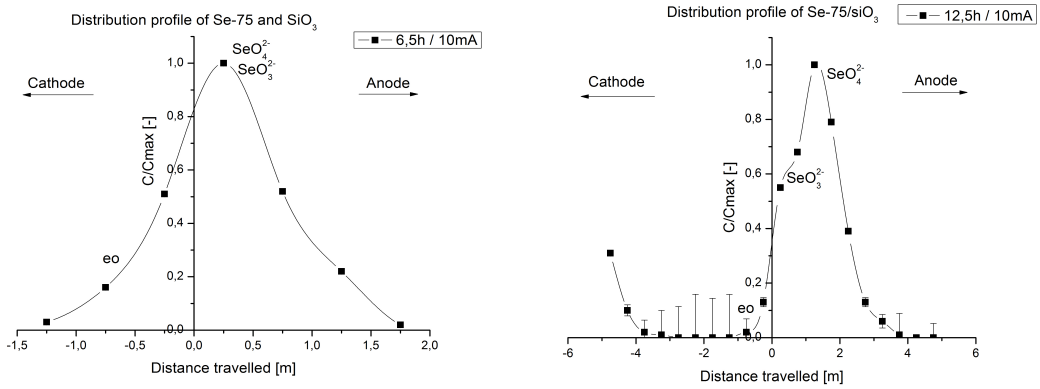


**Figure 29 (left) and 30 (right): Distribution profiles of Se/$SiO_3$-1 (left) and Se/$SiO_3$-3 (right). Experimental time of Se/SiO3-1 was not long enough to create a noticeable separation of selenite and selenate. The highest peak in both profiles can be attributed to selenate. Figure 30 also shows a selenite shoulder near the center. Tails on the cathode side are caused by electroosmotic drag.**

Experiment Se/$SiO_3$-2 showed a 4-peak distribution profile. Upon spotting the selenium tracer on the filter paper in the bentonite core, red precipitate was noticed in the selenium sample indicating precipitate of elemental selenium. Se/SiO3-2 was conducted with a freshly irradiated selenite sample, which was partially reduced by an unidentified contaminant. The distribution profile (figure 31) confirmed this by showing a multiple peak system in which the largest contribution to the total activity remained at the center of the core, indication immobile (sorbed) elemental selenium or immobile selenite. The peak towards the cathode can be attributed to the electroosmotic drag. The small peaks on the right can be assigned to selenate and should be seen as one peak. The bump on the right fits within the error margins of the selenate peak. Elemental selenium remained at the center of clay core. Due to the complexity and the fact that the highest concentration of activity was in the center, the selenate peak had to be isolated in order to determine the apparent velocity and dispersion coefficient.

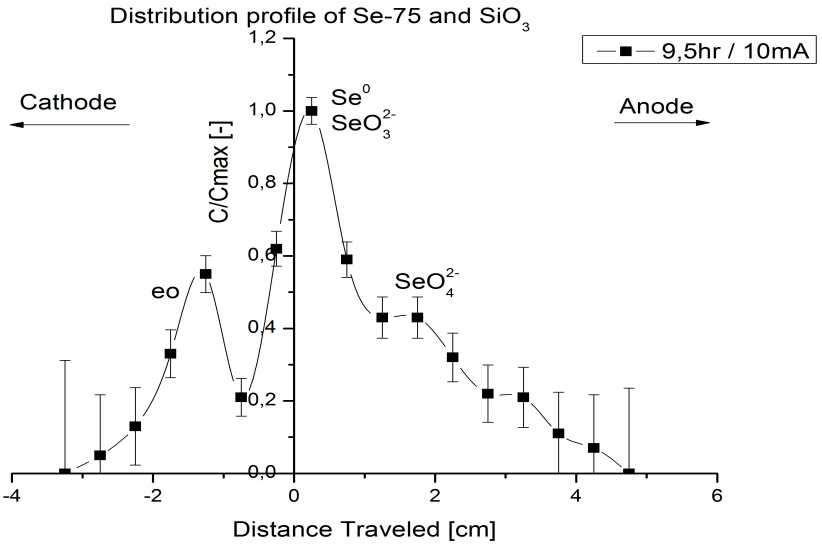


**Figure 31: Distribution profile of Se/$SiO_3$-2. The presence of elemental selenium contributed towards the intensity of the peak at the center of the profile. Selenate was identified towards the right of the center.**

The apparent molecular diffusion coefficient in bentonite found for the selenate in the presence of metasilicate was $3*10^{-10}$ [$m^2/s$], which is identical to the value found without the presence of metasilicate (see figure 32). This indicates that, even though both oxyanions can form outer-sphere complexes, they do not compete for sorption sites.

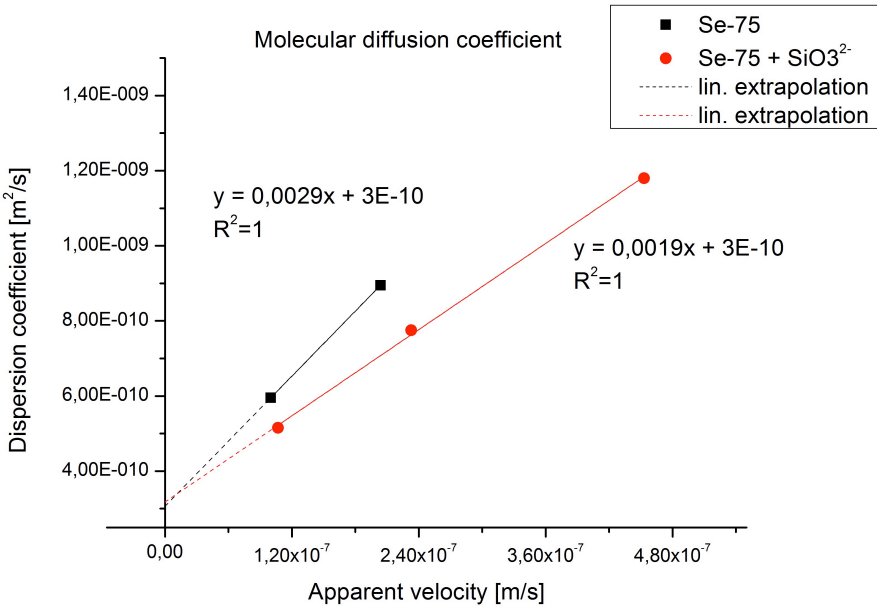


**Figure 32: Apparent molecular diffusion coefficient obtained during selenate (black line) and combined selenate/metasilicate (red line) experiments.**

# 4. CONCLUSIONS AND RECOMMENDATIONS

## 4.1. Conclusions

Five electromigration experiments were conducted to determine the apparent molecular diffusion coefficients of selenate in SBCW saturated bentonite with and without the co-presence of metasilicate. Although selenate and metasilicate resemble each other in their behavior of forming inner-sphere complexes in clays, no competition has been observed between both oxyanions. The apparent molecular diffusion coefficients determined for both situations was $3.0*10^{-10}$ [$m^2/s$], which is only one order of magnitude from literature $3.2*10^{-11}$ [$m^2/s$].

Selenite and selenate have been identified as simultaneously migrating species in the electromigration cell. These two species, and not the influence of hydrogen peroxide, are the cause of the multiple peak distribution profiles. Care must be taken when interpreting the results of electromigration experiments involving redox-sensitive elements.

It has been determined that the phase preference for selenite and selenate is the mobile aqueous clay phase. After separating the solid, gel and liquid phases of the clay sample and analyzing each phase, only little selenium was found in the immobile solid phase, whereas the bulk resided in the mobile liquid and gel phases. The results are according to very mobile nature of selenate.

The use of polycarbonate vials in combination with the electroosmosis of water through bentonite powder is a relatively quick technique for preparing bentonite cores. It ensures easy handling and complete homogeneous saturation. The technique, however, was shown to have little influence on the experimental results in comparison with [17, 29]. Therefore, for future studies, the bentonite cores can be prepared by simply mixing the bentonite powder with the required amount of water, in order to shorten the experimental time. The experimental setup used in this thesis, including the developed core preparation procedures, could be useful for the CEBAMA project, focused on the interaction between clay and concrete interface in the context of geological disposal of radioactive waste.

## 4.2. Recommendations

Because only two experiments have been conducted with selenium as the solitary migrating element, more data points have to be determined in order to get a more accurate apparent molecular diffusion coefficient.

As mentioned in section 1.5.3., cesium will most probably be in the +1 oxidation state when stored in underground repositories and will maintain this oxidation state in the absence of a very strong reducing agent. Because cation exchange is the main retaining factor, it makes sense that other alkali metals can compete for the same exchangeable cations. Sodium, most commonly found in clay as the $Na^+$ ion, for example, is a potential contender for the same sorption spots as cesium ions. Combined experiments with $Cs^+$ and $Na^+$ should therefore be conducted.

Combined experiments with technetium and selenium oxyanions can also be conducted to further research results of [29]. The influence of hydrogen peroxide on the migration behaviour of selenium and technitium should be investigated in this process.

The electromigration cell and the core preparation technique are suitable for the CEBAMA project and other research on migration behavior of ions. Because of the electrically driven migration, data can be acquired within short amounts of time.

## LIST OF REFERENCES


1. Verhoef E., G.J., Poley A., *CORA Disposal concept clay*, 2011, COVRA. p. 2.
2. Grambow, B., *Mobile fission and activation products in nuclear waste disposal.* Journal of Contaminant Hydrology, 2008. **102**(3–4): p. 180-186.
3. Vardon P.J., H.M.A., Fokker P.A., Fokkens J.H., *Technical feasibility of a concept radioactive waste disposal facility in boom clay in the Netherlands*, in *5th International meeting*2012, ANDRA: Montpellier. p. 2.
4. C.C. Allen, M.I.W., *Bentonite in Nuclear Waste Disposal: A Review of Research in Support of the Basalt Waste Isolation Project.* Applied Clay Science, 1988. **3**: p. 11-30.
5. Deer, W.A., R.A. Howie, and J. Zussman, *An introduction to the rock forming minerals*. 1985, London: Longmans.
6. Grauer, R., *Bentonite as a Backfill Material in a High-Level Waste Repository.* MRS Bulletin, 1994. **19**(12): p. 43-46.
7. Heister, K., *Coupled transport in clayey materials with emphasis on induced electrokinetic phenomena*, in *Geosciences* 2005, University Utrecht: Utrecht. p. 120.
8. Maes, N., et al., *The assessment of electromigration as a new technique to study diffusion of radionuclides in clayey soils.* Journal of Contaminant Hydrology, 1999. **36**(3–4): p. 231-247.
9. Yong-Gui Chen, Y.H., Yu-Jun Cui, Wei-Min Ye, *Adsorption of Heavy Metals onto Bentonites Used as Buffer/Backfilling Materials*, in *Unsaturated Soils: Research and Applications*. 2012. p. 385-391.
10. IAEA, *Characterization of swelling clays as components of ethe engineered barrier system for geological repositories*. 2013, Vienna, Austria: International Atomic Energy Anency.
11. Higgo, J.J.W., *Clay as a barrier to radionuclide Migration: a review*. 1986, London: Imperial College.
12. Korkiala-Tanttu, *Bentomap: Survey of bentonite and tunnel backfill knowledge*. Mineralogical and chemical description of the bentonite material. 2009, Finland: VTT Technical Research Centre of Finland.
13. Crini, G. and P.M. Badot, *Sorption Processes and Pollution: Conventional and Non-conventional Sorbents for Pollutant Removal from Wastewaters*. 2010: Presses universitaires de Franche-Comté.
14. Ferris, A.P. and W.B. Jepson, *The exchange capacities of kaolinite and the preparation of homoionic clays.* Journal of Colloid and Interface Science, 1975. **51**(2): p. 245-259.
15. Tuwiner, S.B., W.E. Brown, and L.P. Miller, *Diffusion and Membrane Technology. [By] S.B. Tuwiner. With sections by Lawrence P. Miller ... and W.E. Brown. [With illustrations.]*. 1962, New York; London: Reinhold Publishing Corporation ; Chapman & Hall.
16. S.J., F., *Ideality of clay membranes in osmotic processes: a review.* Clays and Caly Minerals, 1986: p. 214-223.
17. Cannière P., A.M., Thomes Beauwens, Norbert Maes, *Behaviour of Selenium in Boom Clay. State-of-the-art report*, 2010, SCK*CEN: Mol, Belgium.
18. Marivoet, J., & Weetjens, E., *The importance of mobile fission products for long-term seafety in the case of disposal of vitrified high-level waste and*

*spent fuel in a clay formation.* Nuclear Energy Agency of the OECD (NEA): Organisation for Economic Co-Operation and Development - Nuclear Energy, 2009.
19. Bienvenu, P., et al., *A new determination of 79Se half-life.* Applied Radiation and Isotopes, 2007. **65**(3): p. 355-364.
20. Wright, W.G., *Oxidation and mobilization of selenium by nitrate in irrigation drainage.* Enviromental Quality, 1999. **28**: p. 1182 - 1187.
21. Jörg, G., et al., *Preparation of radiochemically pure 79Se and highly precise determination of its half-life.* Applied Radiation and Isotopes, 2010. **68**(12): p. 2339-2351.
22. Ermakov, I.I.N.a.A.N., *Analytical chemistry of selenium and tellurium*. 1972, Jeruzalem: Keter publishing house. 281.
23. Johnson, T.M., *A review of mass-dependent fractionation of selenium isotopes and implications for other heavy stable isotopes.* Chemical Geology, 2004. **204**(3–4): p. 201-214.
24. Bruggeman, C., et al., *Selenite reduction in Boom clay: Effect of FeS2, clay minerals and dissolved organic matter.* Environmental Pollution, 2005. **137**(2): p. 209-221.
25. Beauwens, T., et al., *Studying the migration behaviour of selenate in Boom Clay by electromigration.* Engineering Geology, 2005. **77**(3–4): p. 285-293.
26. R.A. Lidiu, V.A.M., L.L. Andreeva, *Chemical properties of inorganic compounds*. 2000, Russia: Moscow Chemistry. 480.
27. Peak, D., *Adsorption mechanisms of selenium oxyanions at the aluminum oxide/water interface.* Journal of Colloid and Interface Science, 2006. **303**(2): p. 337-345.
28. Scott, M.J. and J.J. Morgan, *Reactions at Oxide Surfaces. 2. Oxidation of Se(IV) by Synthetic Birnessite.* Environmental Science & Technology, 1996. **30**(6): p. 1990-1996.
29. Zappey, J., *The influence of competition on the molecular diffusion coefficient of pertechnetate and selenate in bentonite.* , in *Radiation and Isotopes for Health* 2013, Delft University of Technology: Delft. p. 55.
30. Rosales, E., J.P.G. Loch, and C. Dias-Ferreira, *Electro-osmotic transport of nano zero-valent iron in Boom Clay.* Electrochimica Acta, 2014. **127**(0): p. 27-33.
31. Maes, N., Moors, H., De Cannière, P., Put, M., *Determination of the diffusion coefficient of ionic species by electromigration: feasibility study.* Radiochimica Acta, 1998. **82**: p. 183 - 189.
32. Atkins, P. and J. De Paula, *Physical Chemistry*. 2006: Oxford University Press.
33. M. De Craen, L.W., M. Van Geet, H. Moors, *Geochemistry of Boom Clay pore water at the Mol site*, 2004, SCK.CEN Waste & Disposal Department: Mol, Belgium.
34. Han, D.S., Batchelor, B., Abdel-Wahab, A., *XPS Analysis of Sorption of Selenium(IV) and Selenium(VI) to Mackinawite (FeS).* Wiley Online Library, 2011.
35. Faust, T., *Thermal analysis studies on carbonates, I. aragonite and calcite,* 1950, US geological survey, Washington D.C.
36. Jöhnsson, B., Torbjörn, A., Jönsson, B., *Structure and forces in bentonite MX-80,* 2009, Swedish Nuclear Fuel and Waste Management, Stockholm.

# APPENDICES

## Appendix 1 LabView script for monitoring electrical field

```
<VI syntaxVersion=11 LVversion=12008004 revision=35 name="ReadVoltage.vi">

<TITLE><NO_TITLE name="ReadVoltage.vi"></TITLE>
<HELP_PATH></HELP_PATH>
<HELP_TAG></HELP_TAG>
<RTM_PATH type="default"></RTM_PATH>
<DESC></DESC>
<CONTENT>
	<GROUPER>
		<PARTS>
		</PARTS></GROUPER>
	<CONTROL ID=83 type="Cluster" name="error out">
		<DESC><<B>>error in<</B>> can accept error information wired from VIs previously called. Use this information to decide if any functionality should be bypassed in the event of errors from other VIs.<LF>
<LF>
Right-click the <<B>>error in<</B>> control on the front panel and select <<B>>Explain Error<</B>> or <<B>>Explain Warning<</B>> from the shortcut menu for more information about the error.</DESC>
		<TIP></TIP>
		<PARTS>
			<PART ID=82 order=0 type="Caption"><LABEL><STEXT>error out</STEXT></LABEL></PART>
		</PARTS>
		<CONTENT>
			<GROUPER>
				<PARTS>
				</PARTS></GROUPER>
			<CONTROL ID=79 type="Boolean" name="status">
				<DESC><<B>>status<</B>> is TRUE (X) if an error occurred or FALSE (checkmark) to indicate a warning or that no error occurred.<LF>
<LF>
Right-click the <<B>>error in<</B>> control on the front panel and select <<B>>Explain Error<</B>> or <<B>>Explain Warning<</B>> from the shortcut menu for more information about the error.</DESC>
				<TIP></TIP>
				<PARTS>
					<PART ID=22 order=0 type="Boolean Text"><MLABEL><STRINGS><STRING></STRING><STRING></STRING><STRING></STRING><STRING></STRING></STRINGS></MLABEL></PART>
					<PART ID=82 order=0 type="Caption"><LABEL><STEXT>status</STEXT></LABEL></PART>
				</PARTS>
			</CONTROL>
			<CONTROL ID=80 type="Numeric" name="code">
				<DESC><<B>>code<</B>> is the error or warning code.<LF>
<LF>
Right-click the <<B>>error in<</B>> control on the front panel and select <<B>>Explain Error<</B>> or <<B>>Explain Warning<</B>> from the shortcut menu for more information about the error.</DESC>
				<TIP></TIP>
				<PARTS>
					<PART ID=82 order=0 type="Caption"><LABEL><STEXT>code</STEXT></LABEL></PART>
				</PARTS>
			</CONTROL>
			<CONTROL ID=81 type="String" name="source">
				<DESC><<B>>source<</B>> describes the origin of the error or warning.<LF>
<LF>
Right-click the <<B>>error in<</B>> control on the front panel and select <<B>>Explain Error<</B>> or <<B>>Explain Warning<</B>> from the shortcut menu for more information about the error.</DESC>
				<TIP></TIP>
				<PARTS>
					<PART ID=11 order=0 type="Text"><LABEL><STEXT></STEXT></LABEL></PART>
					<PART ID=82 order=0 type="Caption"><LABEL><STEXT>source</STEXT></LABEL></PART>
				</PARTS>
				<DEFAULT><SAME_AS_LABEL></DEFAULT>
			</CONTROL>
		</CONTENT>
	</CONTROL>
```

```
<CONTROL ID=94 type="Waveform Chart" name="Waveform Chart">
<DESC></DESC>
<TIP></TIP>
<PARTS>
<PART ID=8022 order=0 type="">
<CONTROL ID=231 type="Tree" >
<DESC></DESC>
<TIP></TIP>
<PARTS>
<GROUPER>
<PARTS>
</PARTS></GROUPER>
</PARTS>
<PRIV>
<CELL_FONTS>
[-2 -2]<FONT predef=APPFONT color=000000>
[-1 -2]<FONT predef=APPFONT style='B'
color=000000>
</CELL_FONTS>
<ROW_HEADER>
</ROW_HEADER>
<COL_HEADER>
<STRING>Cursors:</STRING>
<STRING>X</STRING>
<STRING>Y</STRING>
</COL_HEADER>
<STRINGS>
</STRINGS>
</PRIV>
</CONTROL>
</PART>
<PART ID=82 order=0 type="Caption"><LABEL><STEXT>Waveform
Chart</STEXT></LABEL></PART>
</PARTS>
<PRIV>
<PLOTS><STRING>Plot 0</STRING></PLOTS>
<SCALE_NAMES><STRING>Time</STRING><STRING>Amplitude</STRING></SCALE_NAMES>
</PRIV>
</CONTROL>
<CONTROL ID=79 type="Boolean" name="stop">
<DESC></DESC>
<TIP></TIP>
<PARTS>
<PART ID=22 order=0 type="Boolean Text"><MLABEL><FONT predef=SYSFONT
color=FF0000><STRINGS><STRING>STOP</STRING><STRING>STOP</STRING><STRING>STOP</STRING><STRING>S
TOP</STRING></STRINGS></MLABEL></PART>
<PART ID=82 order=0 type="Caption"><LABEL><STEXT><FONT predef=DLGFONT
color=100000C>stop</STEXT></LABEL></PART>
</PARTS>
</CONTROL>
<CONTROL ID=91 type="Path" name="data file:">
<DESC></DESC>
<TIP></TIP>
<PARTS>
<PART ID=8019 order=0 type="Browse Button">
<CONTROL ID=79 type="Boolean" >
<DESC></DESC>
<TIP></TIP>
<PARTS>
</PARTS>
</CONTROL>
</PART>
<PART ID=11 order=0
type="Text"><LABEL><STEXT>c:\users\data\test.bin</STEXT></LABEL></PART>
<PART ID=82 order=0 type="Caption"><LABEL><STEXT>data
file:</STEXT></LABEL></PART>
</PARTS>
<PRIV>
<PROMPT></PROMPT>
<MTCH_PTN></MTCH_PTN>
<PTN_LBEL></PTN_LBEL>
<STRT_PTH><PATH type="absolute"></PATH></STRT_PTH>
<PTH_BTN_LBL></PTH_BTN_LBL>
</PRIV>
```

```
                <DEFAULT>
                        <PATH type="absolute">c<SEP>users<SEP>data<SEP>test.bin</PATH>
                </DEFAULT>
        </CONTROL>
        <CONTROL ID=80 type="Numeric" name="output 1">
                <DESC></DESC>
                <TIP></TIP>
                <PARTS>
                        <PART ID=82 order=0 type="Caption"><LABEL><STEXT>output
1</STEXT></LABEL></PART>
                </PARTS>
        </CONTROL>
</CONTENT>
<BDCONTENT>
        <CONTROL ID=81 type="String Constant" name="format (%.3f)">
                <DESC></DESC>
                <TIP></TIP>
                <PARTS>
                        <PART ID=11 order=0 type="Text"><LABEL><STEXT>%.5f</STEXT></LABEL></PART>
                </PARTS>
                <DEFAULT><SAME_AS_LABEL></DEFAULT>
        </CONTROL>
        <CONTROL ID=81 type="String Constant" name="delimiter (\t)">
                <DESC></DESC>
                <TIP></TIP>
                <PARTS>
                        <PART ID=11 order=0 type="Text"><LABEL><STEXT>,</STEXT></LABEL></PART>
                </PARTS>
                <DEFAULT><SAME_AS_LABEL></DEFAULT>
        </CONTROL>
        <CONTROL ID=79 type="False Constant" name="append to file? (new file:F)">
                <DESC></DESC>
                <TIP></TIP>
                <PARTS>
                </PARTS>
        </CONTROL>
        <NODE ID=197 type="PolyVI" subVIName="Write To Spreadsheet File.vi">
                <DESC></DESC>
        </NODE>
        <NODE ID=47 type="Function" primID=53544446 primName="Format Date/Time String">
                <DESC></DESC>
        </NODE>
        <NODE ID=47 type="Function" primID=20503253 primName="String To Path">
                <DESC></DESC>
        </NODE>
        <NODE ID=62 type="Concatenate Strings">
                <DESC></DESC>
        </NODE>
        <CONTROL ID=81 type="String Constant" >
                <DESC></DESC>
                <TIP></TIP>
                <PARTS>
                        <PART ID=11 order=0 type="Text"><LABEL><STEXT></STEXT></LABEL></PART>
                </PARTS>
                <DEFAULT><STRING>d:\</STRING></DEFAULT>
        </CONTROL>
        <CONTROL ID=81 type="String Constant" >
                <DESC></DESC>
                <TIP></TIP>
                <PARTS>
                        <PART ID=11 order=0 type="Text"><LABEL><STEXT>.csv</STEXT></LABEL></PART>
                </PARTS>
                <DEFAULT><SAME_AS_LABEL></DEFAULT>
        </CONTROL>
        <NODE ID=62 type="Concatenate Strings">
                <DESC></DESC>
        </NODE>
        <CONTROL ID=81 type="String Constant" name="time format string (%c)">
                <DESC></DESC>
                <TIP></TIP>
                <PARTS>
                        <PART ID=11 order=0 type="Text"><LABEL><STEXT></STEXT></LABEL></PART>
                </PARTS>
                <DEFAULT><STRING>%y%m%d%H%M</STRING></DEFAULT>
```

```
		</CONTROL>
		<CONTROL ID=85 type="VISA resource name" name="VISA resource name">
			<DESC></DESC>
			<TIP></TIP>
			<PARTS>
				<PART ID=8017 order=0 type="I/O Name Display">
					<CONTROL ID=148 type="VISA USB Control Out" >
						<DESC></DESC>
						<TIP></TIP>
						<PARTS>
						</PARTS>
					</CONTROL>
				</PART>
			</PARTS>
		</CONTROL>
		<NODE ID=33 type="While Loop">
			<DESC></DESC>
			<BDCONTENT>
				<CONTROL ID=80 type="Numeric Constant" name="milliseconds to wait">
					<DESC></DESC>
					<TIP></TIP>
					<PARTS>
					</PARTS>
				</CONTROL>
				<NODE ID=47 type="Function" primID=54494157 primName="Wait (ms)">
					<DESC></DESC>
				</NODE>
				<CONTROL ID=81 type="String Constant" name="format string">
					<DESC></DESC>
					<TIP></TIP>
					<PARTS>
						<PART ID=11 order=0
type="Text"><LABEL><STEXT>%f</STEXT></LABEL></PART>
					</PARTS>
					<DEFAULT><SAME_AS_LABEL></DEFAULT>
				</CONTROL>
				<NODE ID=146 type="Scan From String">
					<DESC></DESC>
				</NODE>
				<NODE ID=33 type="While Loop">
					<DESC></DESC>
					<BDCONTENT>
						<CONTROL ID=80 type="Numeric Constant" name="y">
							<DESC></DESC>
							<TIP></TIP>
							<PARTS>
							</PARTS>
						</CONTROL>
						<NODE ID=47 type="Function" primID=20205145
primName="Equal?">
							<DESC></DESC>
						</NODE>
						<NODE ID=47 type="Function" primID=42545356 primName="VISA
Read STB">
							<DESC></DESC>
						</NODE>
					</BDCONTENT>
				</NODE>
				<CONTROL ID=81 type="String Constant" name="write buffer">
					<DESC></DESC>
					<TIP></TIP>
					<PARTS>
						<PART ID=11 order=0 type="Text"><LABEL><STEXT>INIT<LF>
FETCH?</STEXT></LABEL></PART>
					</PARTS>
					<DEFAULT><SAME_AS_LABEL></DEFAULT>
				</CONTROL>
				<NODE ID=47 type="Function" primID=54525756 primName="VISA Write">
					<DESC></DESC>
				</NODE>
				<CONTROL ID=80 type="Numeric Constant" name="byte count">
					<DESC></DESC>
					<TIP></TIP>
					<PARTS>
```

```
                                        </PARTS>
                                </CONTROL>
                                <NODE ID=47 type="Function" primID=20445256 primName="VISA Read">
                                        <DESC></DESC>
                                </NODE>
                        </BDCONTENT>
                </NODE>
                <NODE ID=33 type="While Loop">
                        <DESC></DESC>
                        <BDCONTENT>
                                <CONTROL ID=80 type="Numeric Constant" name="y">
                                        <DESC></DESC>
                                        <TIP></TIP>
                                        <PARTS>
                                        </PARTS>
                                </CONTROL>
                                <NODE ID=47 type="Function" primID=20205145 primName="Equal?">
                                        <DESC></DESC>
                                </NODE>
                                <NODE ID=47 type="Function" primID=42545356 primName="VISA Read STB">
                                        <DESC></DESC>
                                </NODE>
                        </BDCONTENT>
                </NODE>
                <CONTROL ID=81 type="String Constant" name="write buffer">
                        <DESC></DESC>
                        <TIP></TIP>
                        <PARTS>
                                <PART ID=11 order=0 type="Text"><LABEL><STEXT></STEXT></LABEL></PART>
                        </PARTS>
                        <DEFAULT><STRING>*ESE 1<LF>
CONF:VOLT:DC<LF>
TRIG:SOUR IMM<LF>
*OPC</STRING></DEFAULT>
                </CONTROL>
                <NODE ID=47 type="Function" primID=54525756 primName="VISA Write">
                        <DESC></DESC>
                </NODE>
                <CONTROL ID=81 type="String Constant" name="write buffer">
                        <DESC></DESC>
                        <TIP></TIP>
                        <PARTS>
                                <PART ID=11 order=0 type="Text"><LABEL><STEXT></STEXT></LABEL></PART>
                        </PARTS>
                        <DEFAULT><STRING>*CLS</STRING></DEFAULT>
                </CONTROL>
                <NODE ID=47 type="Function" primID=534C4356 primName="VISA Close">
                        <DESC></DESC>
                </NODE>
                <NODE ID=47 type="Function" primID=54525756 primName="VISA Write">
                        <DESC></DESC>
                </NODE>
                <NODE ID=47 type="Function" primID=524C4356 primName="VISA Clear">
                        <DESC></DESC>
                </NODE>
</BDCONTENT>
</VI>
```

## Appendix 2 MatLab script for fitting experimental data

```
clc;
clear all;
close all;

M=;                 % s-1    (insert initial amount of activity)
S=;                 % m2     (insert surface of the clay slices)
t=;                 % s      (insert time in secondes)
x_aangebracht =;    % cm     (insert location where tracer is spiked, if done
                                correctly this should be the middle (0))

% use the correct interpunction (dot/comma)
% insert x in centimeters
% below: Enter the location of the slices. Mind the matrix dimension.
x=[];
x=x./100;

% normalize the activity by dividing A through A(max) and enter below
c_norm=[];

% the next codes are to calculate the Vapp and Di
maxC=max(c_norm);
maxi=find(c_norm == maxC);
maxX=x(maxi);
Vapp=(maxX-x_aangebracht*0.01)/t;

options=optimset('Display','on');
Di0=1e-10;
x0=[Di0];

[fitx]=fminsearch(@formule,x0,options,x,c_norm,M,S,t,Vapp);
Di=fitx(1)
Vapp

c_calc=(M./(2.*S.*sqrt(pi.*Di.*t))).*exp(-((x- Vapp.*t).^2)./(4.*Di.*t));
c_calc=c_calc/max(c_calc);

E=sum((c_calc-c_norm).^2);

figure;
plot(x,c_norm,'-*',x,c_calc,'-o');
legend('measured','calculated');
ylabel('c/c_0');
xlabel('x [m]');

end

function E=formule(fitx,x,c_norm,M,S,t,Vapp)

Di=fitx(1);

c_calc=(M./(2.*S.*sqrt(pi.*Di.*t))).*exp(-((x-Vapp.*t).^2)./(4.*Di.*t));
c_calc=c_calc/max(c_calc);

% Compute the error in each concentration
E=sum((c_calc-c_norm).^2);
end
```

## Appendix 3 Bentonite core preparation

Goal

To prepare two homogeneous, 5 cm long, bentonite cores with diameter of 28 mm.

Experimental procedures

1. Grease the inside of the sample holder in the electromigration cell to prevent water from flowing between the sample holder and the outside edge of the polycarbonate vials.

2. Insert two 5 cm polycarbonate vials into the sample holder of the electromigration cell. Seal the cathode end with a glass filter.

3. Fill 9.5 cm of the sample holder with bentonite powder. Add 1 mL of SBCW every 1.0 cm to ensure initial conductivity in the core.

4. Seal the anode compartment with the second glass filter and close both electrolyte compartments with the electrode lids.

5. Assemble the rest of the cell and connect the peristaltic pumps to the cell.

6. Fill both electrolyte compartments with SBCW.

7. Apply 10 - 15 mA to the cell.

8. Check every hour for flooding and measure pH and electric field.

9. Turn DC-power supply off after saturation has completed (after approximately 24 hours) and drain electrolyte compartments.

10. Remove the glass filters and push the polycarbonate vials with the saturated bentonite core inside out.

## Appendix 4 Electromigration experiment with radionuclides

Experimental procedures

1. Grease the inside of the sample holder in the electromigration cell to prevent water from flowing between the sample holder and the outside edge of the polycarbonate vials.

2. Insert one 5 cm polycarbonate vial with a saturated core into the sample holder of the electromigration cell (cathode side). Seal the cathode end with a glass filter.

3. Insert two electrode needles into the core.

4. Lay circular filter paper (26 mm diameter) at the center of the sample holder on top of the already inserted 5 cm of saturated core.

5. Wet the filter paper with 36 µL of SBCW and Spike the filter paper with 150 - 250 kBq of activity.

6. Insert the second polycarbonate vial with a saturated core into the sample holder of the electromigration cell (anode side). Seal the anode end with a glass filter.

7. Close both electrolyte compartments and assemble the rest of the electromigration cell. Connect peristaltic pumps with the cell.

8. Fill both compartments with SBCW.

9. Apply current and voltage for designated time periode. Check every hour for flooding and measure pH and the potential over the clay core.

10. After x hours, turn DC-power supply off and drain electrolyte compartments. Disassemble the cell.

11. Push the polycarbonate vials with the clay core inside out of the cell and let them dry for 2 hours. After two hours push the core out of the polycarbonate vials.

12. Cut the core in 5 mm slices with a spatula and put each slice in a 50 mL plastic vial. Add 40 mL of milli-q to each vial. Close plastic vials and seal with parafilm.

13. Rotate overnight.

14. Transfer 10 mL solution from each vial to a glass scintillation vial compatible for the γ-detector.

## Appendix 5 Separation of selenite and selenate ions

Experimental procedures

1. Dissolve 25 mg $NaSeO_2$ in 40 mL 0.1 M NaOH solution to obtain a $5.85*10^{-3}$ M Se (IV) solution.

2. Pipet 2.0 mL solution in to a 15 mL plastic vial and add 2.22 mg of thiourea ($CH_4N_2S$). Shake the solution a few minutes. Thiourea is a reducing agent which reduces Se(IV) to, red, elemental selenium.

3. Centrifuge the red suspension for 20 minutes at 3900 rpm and pipet the supernatant into a new 15 mL plastic vial.

4. Add 2.22 mg of thiourea to the solution, vortex for 30 seconds and wait for 20 minutes. Check for red precipitation. Centrifuge again if any red precipitation occurs.

5. Repeat step 5 until no red precipitation forms when adding thiourea.

6. Measure selenate concentration with ICP.

## Appendix 6 Synthetic boom clay water

General

Boom Clay pore water is basically a $NaHCO_3$ solution of 15 mM. A 15 mM $NAHCO_3$ solution can thus be used in the experiments.

Preparation of SBCW

The directives for the preparation of Synthetic Boom Clay Water have been published by Maes *et al.* (2000 and 2004).

If you are planning to work in anaerobic conditions, make sure your water is degassed! Always leave the bottle open in the glovebox, to allow the last ppm $O_2$ to diffuse out. Be aware of the oxygen level while you do that. Then, close the bottle.

To prepare 1 L of synthetic clay water, add the following products to 1 L of high quality water (demineralised, bidistilled, milli-q,...):

**Table 6: Weight of salts needed for the preparation of 1 L of SBCW.**

| Salt | Quantity (mg) | MW | (Mole/L) |
|---|---|---|---|
| $NaHCO_3$ | 1170 | 83.996 | 1.39E-02 |
| $H_3BO_3$ | 43 | 61.834 | 6.95E-04 |
| KCl | 25 | 74.555 | 3.35E-04 |
| $MgCl_2 \cdot 6\ H_20$ | 22 | 203.218 | 1.08E-04 |
| NaF | 11 | 41.988 | 2.62E-04 |
| NaCl | 10 | 58.443 | 1.71E-04 |
| $FeCl_2$ | 3 | 126.751 | 2.37E-05 |
| $Na_2SO_4$ | 0,3 | 142.041 | 2.11E-06 |
| | | | |
| **TDS** | **1284.3** | **-** | **1.55E-02** |

TDS: Total Dissolved Salts

- Supersaturation with 1000 mg $CaCO_3$ to adjust $Ca^{2+}$, followed by one week of stirring.
- Bubbling with 0.4 $CO_2$ % gas mixture until constant pH (carrier gas Argon of $N_2$).
- Always filter through a 0.22 µm filter before use. In case of solubility experiments, perform an ultrafiltration through a 30000 MWCO filter.
- Bubbling with 0.4 $CO_2$ % gas mixture until constant pH.

## Appendix 7 Detailed observations of clay core preparation trials

In the first trial the sample holder was simply filled with bentonite powder and sealed with two glass filters. By pipetting small amounts of SBCW in the electrode openings, initial conductivity was established. Saturation took approximately 100 hours and many issues had occurred in that time. 1) The glass filter, sealing the sample holder from the electrolyte compartment, cracked due to pressure from the swelling bentonite and/or pressure exerted by negatively charged clay particles that are attracted towards the anode. 2) Iron and clay particles, presumably colloids, that diffused through (or around) the glass filters, precipitated in the anode compartment. This contaminated the compartment and changed the molecular structure of the bentonite. 3) At first conductivity, and thus electroosmosis, was very low. It was believed that high current and high electrical field were the hart of the last two problems. The slow increase in conductivity was attributed to the lack of SBCW in the initial powder.

The second trial was therefore conducted under less current. During the filling of the sample holder with bentonite powder, a drop of SBCW was added every 5 mm. The effects were positive. The filter had survived and preparation time was halved. However, after a peristaltic pump failed overnight, pH wasn't neutralized and a large pH gradient set in. The failing of the peristaltic pump exposed the difficulties of leaving the experiment run overnight (electrically controlled by LabView). New peristaltic pumps were acquired.

In the first two trials removing the core from the cell was simple (figure 33). Inserting it back into the sample holder for the active experiment, without damaging the homogeneity, on the other hand, was troublesome. By using polycarbonate vials (see figure 34) to encapsulate the bentonite powder while saturating, the core stayed untouched when removed from and inserted back into the cell core. Polycarbonate vials were used in all future core preparations.

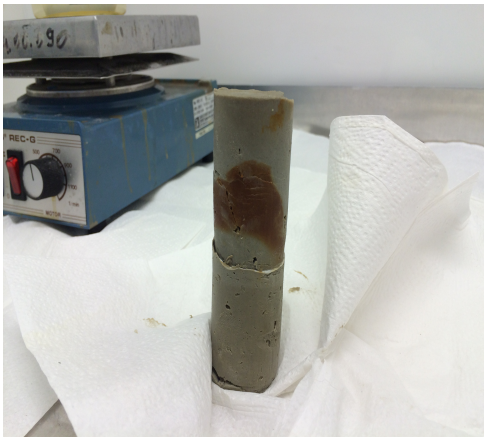

Figure 33: Saturated claycore without the use of polycarbonate vials.

Figure 34: Saturated claycore in a polycarbonate vial.

The third trial was conducted with the same proceedings as the second, except for the polycarbonate vial and an even lower current. As expected, preparation time was slightly longer (due to the lower current) and the core stayed untouched and homogeneous during all actions.

In the final trial the low current was maintained in order to preserve the molecular composition of the clay and to relieve pressure from the filters. Experimental time was halved again by heavily wetting the powder every 5mm when filling the sample holder.